A coherent feed-forward-loop in the Arabidopsis root stem cell organizer regulates auxin biosynthesis and columella stem cell maintenance

Mohan Sharma
1Signalling Research Centres BIOSS and CIBSS, Faculty of Biology, University of Freiburg, Schänzlestrasse 1, 79104 Freiburg, Germany https://orcid.org/0000-0001-5594-5210

Thomas Friedrich
1Signalling Research Centres BIOSS and CIBSS, Faculty of Biology, University of Freiburg, Schänzlestrasse 1, 79104 Freiburg, Germany

Federico Peruzzo
1Signalling Research Centres BIOSS and CIBSS, Faculty of Biology, University of Freiburg, Schänzlestrasse 1, 79104 Freiburg, Germany

Vikram Jha
1Signalling Research Centres BIOSS and CIBSS, Faculty of Biology, University of Freiburg, Schänzlestrasse 1, 79104 Freiburg, Germany

Limin Pi
Institute for Advanced Studies, Wuhan University, No. 299 Bayi Road, 430072 Wuhan, China

Edwin Philip Groot
1Signalling Research Centres BIOSS and CIBSS, Faculty of Biology, University of Freiburg, Schänzlestrasse 1, 79104 Freiburg, Germany

Noortje Kornet
1Signalling Research Centres BIOSS and CIBSS, Faculty of Biology, University of Freiburg, Schänzlestrasse 1, 79104 Freiburg, Germany

Marie Follo
Uniklinik Freiburg, Zentrum für Translationale Zellforschung (ZTZ), Breisacher Straße 115, 79106 Freiburg, Germany

Ernst Aichinger
1Signalling Research Centres BIOSS and CIBSS, Faculty of Biology, University of Freiburg, Schänzlestrasse 1, 79104 Freiburg, Germany

Christian Fleck
Freiburg Center for Data Analysis and Modeling (FDM), Ernst-Zermelo-Str. 1, 79104 Freiburg, Germany

Thomas Laux (laux@biologie.uni-freiburg.de)
1Signalling Research Centres BIOSS and CIBSS, Faculty of Biology, University of Freiburg, Schänzlestrasse 1, 79104 Freiburg, Germany https://orcid.org/0000-0001-6659-0515

Research Article

Keywords: Root stem cells, WOX5, HAN, QC signaling, transcriptional regulation

Posted Date: December 12th, 2023

DOI: https://doi.org/10.21203/rs.3.rs-3738114/v1

Additional Declarations:
Competing interests: The authors declare no competing interests.

A coherent feed-forward-loop in the *Arabidopsis* root stem cell organizer regulates auxin biosynthesis and columella stem cell maintenance

Mohan Sharma[1], Thomas Friedrich[1], Federico Peruzzo[1], Vikram Jha[1], Limin Pi[2], Edwin Philip Groot[1], Noortje Kornet[1], Marie Follo[3], Ernst Aichinger[1], Christian Fleck[4], and Thomas Laux[1,5*]

Affiliations:

[1]Signalling Research Centres BIOSS and CIBSS, Faculty of Biology, University of Freiburg, Schänzlestrasse 1, 79104 Freiburg, Germany.

[2] Present address: Institute for Advanced Studies, Wuhan University, No. 299 Bayi Road, 430072 Wuhan, China

[3] Uniklinik Freiburg, Zentrum für Translationale Zellforschung (ZTZ), Breisacher Straße 115, 79106 Freiburg, Germany

[4] Freiburg Center for Data Analysis and Modeling (FDM), Ernst-Zermelo-Str. 1, 79104 Freiburg, Germany

[5] Sino-German Joint Research Center on Agricultural Biology, Shandong Agricultural University, Tai'an, Shandong, China.

*Corresponding author: laux@biologie.uni-freiburg.de; Tel.: +49 761 203-2943; Fax.: +49 761 203-2745

Abstract

Stem cells in the plant meristems are kept undifferentiated by signals from surrounding cells and provide the basis for continuous organ formation. In the stem cell organizer of the *Arabidopsis thaliana* root, the Quiescent Center (QC), the WOX5 transcription factor functions as a central hub in regulating columella stem cell (CSC) homeostasis. However, the processes mediating WOX5 function have yet to be discovered. Here, we identify the transcription factor HAN as a central mediator of WOX5-regulated stem cell maintenance. *HAN* is required and sufficient to maintain CSCs undifferentiated and to induce ectopic stem cells. WOX5 and HAN repress transcription of the differentiation factor gene *CDF4* in a coherent Feed Forward Loop (cFFL), one output of which is the expression of the auxin biosynthesis gene *TAA1* and maintaining auxin response maxima in the organizer. Mathematical *WOX5/HAN/CDF4* cFFL modeling suggests a mechanism to buffer columella stem cell maintenance against input noise.

Maintenance of stem cell pluripotency in plants and animals employs similar strategies, including signaling from the surrounding tissues that provide repression of differentiation pathways in the stem cells[1-3]. Plant stem cells are localized in organized niches called meristems, enabling them to form new organs throughout life. In his seminal work on the root meristem about seven decades ago, Frederick Clowes[4,5] recognized a group of cells with a reduced mitotic activity that he termed the quiescent center (QC), and that is surrounded by "initials" (stem cells) from which all cells types of the root are derived. Elegant cell ablation experiments in *Arabidopsis* suggested the concept of the QC as the stem cell organizer of the root meristem[6]. Subsequent genetic analyses revealed a complex network of hormones, transcription factors, redox state, and signaling pathways that regulate QC identity, the communication between QC and stem cells, and the maintenance of stem cells (for review:[1,7,8]).

Stem cell organizers in the shoot, root, and vascular meristems express specific WUSCHEL-related homeobox (WOX) genes of the evolutionary youngest WUSCHEL-clade to maintain stem cells undifferentiated (for review:[1]). Furthermore, members of the ancient WOX13 clade are associated with stem cell regeneration in the basal moss *Physcomitrium patens*[9], suggesting WOX genes as universal regulators of plant stem cells. In the *Arabidopsis* QC, which typically comprises about 4-8 cells, the WOX5 transcription factor functions as a regulatory hub, integrating many regulatory inputs[7]. As one output, WOX5 directly downregulates the expression of *Cyclin D3;3* to keep the QC cells in a relatively quiescent state[10], and this regulation is thought to involve direct interaction with the transcription factors BRASSINOSTEROIDS AT VASCULAR AND ORGANIZING CENTER (BRAVO) and PLETHORA3 (PLT3)[11,12]. In addition to its cell-autonomous function on QC quiescence, WOX5 is essential for QC signaling to keep the underlying (distal) layer of columella stem cells (CSCs) undifferentiated and redundantly with other factors, also the proximal stem cells

that give rise to vascular and ground tissues [13,14]. The distal daughter cells of CSC divisions differentiate directly into columella cells (CC) that accumulate starch grains for gravity sensing, whereas the proximal daughter cells replenish the CSCs. WOX5 promotes CSC pluripotency in part by directly downregulating transcription of the differentiation gene *CYCLING DOF FACTOR 4* (*CDF4*) through recruiting the Groucho/TUP1-type co-repressor TOPLESS/TOPLESS RELATED and HISTONE DEACETYLASE 19 to the *CDF4* promoter and removing transcriptional-competent-chromatin associated histone depositions H3K9Ac and H3K14Ac[14].

Several studies indicate a pivotal role of directional transport of the phytohormone auxin and an auxin response maximum in the QC in regulating *WOX5* expression[15] and root meristem maintenance[16,17]. However, grafting wild-type shoots on roots largely deficient in auxin biosynthesis did not restore the auxin response maximum in the QC nor stem cell maintenance. In contrast, expression of the auxin biosynthesis gene *TRYPTOPHAN AMINOTRANSFERASE OF ARABIDOPSIS 1* (*TAA1*) in the QC did[18], suggesting an important role of auxin biosynthesis in the stem cell organizer rather than shoot-derived auxin in root meristem regulation.

The GATA3-type transcription factor *HANABA TARANU* (*HAN)* functions in several processes that are associated with the control of developmental boundaries, including the boundaries separating proembryo from suspensor, shoot meristem from lateral organs, and individual floral organs from each other[19,20]. However, a role in stem cell regulation has not yet been reported.

WOX5 protein can move from the QC into the CSC layer, resulting in two opposing gradients of the stemness factor WOX5 and the differentiation factor *CDF4* in the CSC niche[14]. However, a recent study suggests that WOX5 movement is not indispensable for CSC maintenance[21]. Therefore, we hypothesized that *WOX5* controls additional undiscovered downstream pathways in stem cell control. Here, we use transcriptional profiling of *WOX5*-induced ectopic CSC-like stem cells to search for novel CSC regulators. We identified *HAN* as a central mediator of WOX5 in a coherent Feed-Forward-Loop network to regulate stemness in the root stem cell niche and during de novo stem cell induction.

Results

WOX5 upregulates *HAN* transcription during ectopic stem cell induction

To identify processes that act downstream of *WOX5* in regulating stem cell fate, we used induction of *35S:WOX5-GR* by application of dexamethasone (DEX), which causes accumulation of cells that are indistinguishable from CSCs concerning their relatively small size, the absence of starch accumulation (**Fig. 1a-b**), expression of the CSC marker *J2341* and downregulation of the differentiated columella cell (CC) marker *Q1630/Q0680*[14]. We, therefore, named these cells "induced CSCs" (iCSCs). To determine the transcriptional changes during this event, we isolated protoplasts of CCs marked by *Q0680:erGFP* expression (**Fig. 1c**) via fluorescent-activated protoplast sorting. The *HAN* gene, encoding a GATA3-type Zinc Finger transcription factor, was the most strongly upregulated gene with an 8-9-fold increase at one and four hours after induction of *35S:WOX5-GR* (**Fig. 1d**). We confirmed that induction of *35S:WOX5-GR* activates *HAN* transcription during iCSC formation, by the upregulation of a *pHAN:NLS-3xYFP* reporter that harbors nuclear-localized 3xYFP driven from a 7.1 kb DNA fragment upstream of the HAN coding sequence (**Fig. 1e-f)**. Furthermore, we observed that increased *HAN* mRNA levels after inducing *35S:WOX5-GR* expression were abolished by adding the protein biosynthesis inhibitor cycloheximide, indicating that the regulation is indirect (**Fig. 1i**).

When constructing the *pHAN:NLS-3xYFP* reporter, we identified a 531 bp-long fragment -5196bp/-4608bp upstream of the predicted ATG start codon that is essential for the response to *35S:WOX5-GR* (**Fig. 1g-h)** and we further delineated the WOX5-responsive element to the region between -4911 and -4608bp (**Extended Data Fig. 1a-d**). This finding was surprising because distal regulatory elements that control transcription from such a long distance are commonly found in animals but are less known in plants[22-25]. Histone H3K9 acetylation was significantly increased at this site upon WOX5 induction (**Extended Data Fig. 1e-f**), opposite

to the WOX5-induced chromatin changes on its direct target *CDF4*[14]. We also noticed increased *pHANΔ:nls3xYFP* expression in lateral regions of the root tip compared to the non-mutated reporter (compare **Fig. 1g-h**), suggesting the presence of additional cell type-specific regulatory sites within the deleted 531 bp fragment, which was not investigated further.

Together, these data suggest that during iCSC formation, the WOX5 protein indirectly activates the transcription of the *HAN* gene through a distal regulatory element.

HAN is essential and sufficient for *WOX5*-induced ectopic stem cell formation

To address whether *HAN* function is essential for *WOX5*-induced iCSC formation, we induced *35S:WOX5-GR* in the *han-30* mutant[26] and observed a strong suppression of iCSC formation (**Fig. 2a-c)** compared to *35S:WOX5-GR* expression in the wild-type background. This indicates that WOX5 activity requires HAN for iCSC formation. Conversely, we asked whether overexpression of *HAN* alone can trigger iCSC formation. Indeed, induction of *HAN* overexpression resulted in the formation of several layers of CSC-like cells at the position of CCs, as indicated by the small cell size, the absence of starch granules, the absence of *Q0680* CC marker expression (**Fig. 2d**), and the expanded expression domain of the *J2341* CSC marker (**Fig. 2e**). These phenotypical changes are strikingly similar to the ones caused by overexpression of *WOX5* (**Fig. 2f-g**)[14].

From these data, we conclude that *HAN* plays a major role in mediating *WOX5* function in iCSC formation.

HAN mediates *WOX5* function in the columella stem cell niche

We then asked whether HAN can also mediate *WOX5* function in the genuine CSC niche. Indeed, we found that the *han-30* loss-of-function mutant accumulates starch granules at the CSC and, to a lesser extent, the QC positions, indicative of CC differentiation (**Fig. 3a-c, f, h**) and highly similar to the *wox5-1* mutant (**Fig. 3d, f, h**). Furthermore, *han-30* roots lacked detectable levels of expression of the CSC marker *J2341* (**Fig. 3j-k**), again similar to the *wox5-1* mutant[14]. Expressing the *HAN* cDNA from the beforementioned 7.1kb *HAN* upstream fragment entirely suppressed the CSC niche defects of the *han-30* loss-of-function mutant (**Extended Data Fig. 2a-b**), confirming that the *han-30* mutation causes these defects. Furthermore, the *han-30* defects in the columella stem cell niche are similar to the ones we detected in the null allele *han-1*, suggesting that *han-30* is an amorphic allele (**Extended Data Fig. 2c-e**).

In addition to regulating stem cell maintenance, *WOX5* is required to repress the frequency of QC cell divisions[10]. We also observed increased cell division activity compared to the wild type in the *han-30* mutant **(Fig. 3g, i)**. However, in contrast to *wox5-1,* where expression of the QC marker QC184 is undetectable in all roots (**Fig. 3d**), about 40% of *han-30* roots still express the QC184 (n>60 in three independent experiments, **Fig. 3b-c** and **Table S1**), suggesting the requirement of additional downstream pathways for a subset of *WOX5* functions. Furthermore, the *wox5-1 han-30* double mutant was indistinguishable from the *wox5-1* single mutant regarding QC division, absence of QC184 expression, and CSC maintenance defects (**Fig. 3e-i**), consistent with *HAN* acting downstream of *WOX5* in the CSC niche.

To address this model at the molecular level, we asked whether the far lower endogenous levels of *WOX5* in the CSC niche, compared to overexpression of *WOX5* in iCSC formation, can also upregulate *HAN* transcription. In wild-type roots, we detected a strong *pHAN:NLS-3xYFP* signal in the stele and, at a weaker level, in QC and CSC cells (insets in **Fig. 4a, c**; **Table S2**).

By contrast, *pHAN:nls3xYFP* expression was undetectable at the QC and CSC positions in *wox5-1* (**Fig. 4b, c**; **Table S2**). Importantly, deleting the 531bp-long fragment from the *HAN* promoter, which is necessary for its upregulation during *WOX5*-triggered iCSC formation, resulted in a complete loss of its expression in QC and CSC of wild-type roots (**Fig. 4c**). Thus, the endogenous levels of WOX5 in the genuine stem cell niche and the WOX5-response region at -4,85kb are required for *HAN* expression in the QC and CSC, suggesting that similar molecular mechanisms regulate the endogenous CSC niche and the induction of ectopic stem cells.

We then asked whether *HAN* function mediates *WOX5* regulation of the stem cell niche. To this end, we expressed *HAN* from an inducible *WOX5* promoter system denoted as *pWOX5>>HAN* (*pWOX5:Gal4-VP16-GR; UAS:HAN; UAS:erDsRed*) in the *wox5-1* mutant. DEX-induction of *HAN* expression with this construct was specific for the QC as indicated by the linked *UAS:erDsRed* reporter (**Extended Data Fig. 3a**). *pWOX5>>HAN* re-established wild-type-like CSCs in the *wox5-1* background with one or two layers of starch-free cells underneath the QC (**Fig. 4d-f, Extended Data Fig. 5a-b** and **Table S3**). Furthermore, this layer did not express the QC markers QC25 (**Fig. 4e**) or *pWOX5:nlsGUS (***Fig. 4f)**, suggesting that it does not consist of additional QC cells. In control experiments, *pWOX5>>HAN* expression did not cause any changes in the Col-0 wild-type background (**Extended Data Fig. 3b**). DEX application did not cause any changes in root morphology or marker gene expression in the absence of the *HAN* transgene (**Extended Data Fig. 3c-f**), confirming that QC-expressed *HAN* complemented the lack of *WOX5* activity in the CSC maintenance.

Notably, whereas *pWOX5>>WOX5* expression restored the expression of QC184 in about half of all roots (**Fig. 4g, i**), this was only rarely observed for *pWOX5>>HAN* (**Fig. 4d, i**), despite comparable expression levels of the tandem DsRed reporter (**Extended Data Fig. 4**).

Furthermore, *pWOX5>>HAN* did not suppress ectopic QC-division in *wox5-1* (**Extended Data Fig. 5a-c**).

These results suggest that *HAN* is a major promoter of CSC stemness downstream of *WOX5*, whereas it cannot fully complement all *WOX5* functions within the QC.

HAN negatively regulates the transcription of the differentiation gene *CDF4*

To gain insight into how HAN regulates the columella stem cell niche, we addressed the relationship between *HAN* and *CDF4*, a crucial direct target of WOX5 in maintaining the CSC niche[14]. Indeed, we found that *35S:HAN-GR* induction strongly suppressed *pCDF4:NLS-3xYFP* expression (**Fig. 5a-c**). Furthermore, *pCDF4:NLS-3xYFP* expression was upregulated at the QC position in the *han-30* mutant compared to the wild type (insets in **Fig. 5d-e**). Because WOX5 directly binds to the *CDF4* promoter to repress its transcription[14], we wondered whether HAN might downregulate *CDF4* transcription by inducing *WOX5* expression. However, refuting this possibility, we did not detect any upregulation of *pWOX5:erCFP* upon *35S:HAN-GR* induction (**Extended Data Fig. 6a-c).** Furthermore, we found that the repression of *CDF4* by HAN is unaffected by inhibition of protein biosynthesis, indicating that no production of an intermediate protein is required (**Fig. 5f**). Finally, we detected binding of HAN to the *CDF4* promoter by ChIP-PCR centering two predicted GATA-binding motifs of HAN (**Fig. 5g-h**). These results suggest that HAN directly represses *CDF4* transcription.

To estimate the contribution of HAN to the WOX5-mediated repression of *CDF4*, we compared the repression of *CDF4* mRNA levels by *35S:WOX5-GR* in wild-type and *han-30* backgrounds. We found that the *han-30* mutation ameliorated the downregulation of *CDF4* expression by WOX5 to about 50% (**Fig. 5i**).

These results suggest that the *WOX5/HAN/CDF4* module constitutes a coherent Feed-Forward Loop (cFFL) in columella stem cell regulation, with the *CDF4* promoter being the integrator of direct repressive WOX5 and HAN inputs.

Local auxin biosynthesis in the QC is an output of the *WOX5/HAN/CDF4* cFFL

To study the physiological outputs of this cFFL, we considered auxin, which is essential for CSC regulation[15-17,27,28]. In line with this hypothesis, we found that inhibition of auxin response in the QC through expressing the dominant-negative bodenlos (bdl) protein mimicked the stem cell defects of *wox5-1/han-30* (**Extended Data Fig. 7a-d**). Furthermore, mutants of the auxin biosynthesis genes *TRYPTOPHAN AMINOTRANSFERASE OF ARABIDOPSIS (TAA1)* and related *(TAR1)* displayed CSC termination similar to the *wox5-1/han-30* mutants (**Extended Data Fig. 7e-g, Fig. 3f-h**) and repressed *WOX5*-mediated iCSC formation (**Extended Data Fig. 7h-j**).

To address whether auxin homeostasis might be targeted by the *WOX5/HAN/CDF4* cFFL, we analyzed the expression of reporter genes for auxin response (*DR5:GFP*) and biosynthesis (*pTAA1:GFP-TAA1*). In the wild-type root meristems, *DR5:GFP* expression shows an expression gradient with the maximum in the QC (**Fig. 6a**) where also the expression of the *pTAA1:GFP-TAA1* reporter peaks[29] (**Fig. 6b**). By contrast, expression of both reporters was strongly reduced in the *han-30* (**Fig. 6c-d, m-n**), similar to the previously studied *wox5-1* mutant[27,28] (**Fig. 6e-f, o-p**). Furthermore, we found that the *han-30* mutation ameliorated the upregulation of *pTAA1:GFP-TAA1* by *35S:WOX5-GR* (**Fig. 6q**), similar to its effect on *WOX5*-mediated repression of *CDF4*.

We then analyzed whether auxin homeostasis might be targeted by the *WOX5/HAN/CDF4* cFFL through *CDF4* as its integrator. Indeed, we found that *35S:CDF4-GR* induction strongly

239 reduced *DR5:GFP* and *pTAA1:GFP-TAA1* expression levels (**Fig. 6i-j, o-p, r**), oppositely to
240 the effects of *35S:WOX5-GR* induction[28] (**Fig. 6g-h**). Furthermore, *pWOX5:CDF4* strongly
241 reduced expression from both reporters specifically in the QC (**Fig. 6k-l, o-p**), mimicking the
242 effects of the *han-30* and *wox5-1* mutants (**Fig. 6c-f**).
243
244 These results suggest auxin biosynthesis in the QC as an output of the *WOX5/HAN/CDF4* cFFL
245 in columella stem cell regulation (**Fig. 6s**).

Discussion:

Stem cell homeostasis in plant meristems requires the integration of multiple developmental and environmental cues. *WOX5* is a central hub in coordinating columella stem cell maintenance, and its ectopic expression can cause the formation of iCSCs. However, the processes determining the output of WOX5 activity are largely unknown. Here, we report that CSC maintenance is regulated by a *WOX5/HAN/CDF4* cFFL with local auxin biosynthesis in the stem cell organizer as an essential output. In the following, we discuss the implications of this model in columella stem cell regulation.

Classical laser ablation experiments demonstrated that maintenance of the columella stem cells requires a signal from the overlying QC, establishing the concept of stem cell regulation by stem cell organizing cells in plants [6]. The QC expresses the *WOX5* gene, but the WOX5 protein can move from the QC to the underlying cell layer, where it represses *CDF4* and maintains CSCs undifferentiated[14]. Still, evidence also suggests yet unknown factors downstream of *WOX5* as potential signals controlling CSC stemness[21]. Because transgenic expression of *HAN* in the QC region of the *wox5-1* mutant restored CSC maintenance in the underlying cell layer, it appears, therefore, that the WOX5-cFFL in QC-CSC signaling involves at least two non-cell-autonomous components, mobile WOX5 protein, and a HAN-dependent signal. Our results indicate the upregulation of auxin biosynthesis as an output of the cFFL, making auxin a candidate for this signal. This finding agrees with elegant experiments showing that local *TAA1* expression in the QC can restore the root stem cell niche including CSCs in the *taa1 tar2* auxin biosynthesis mutant without requiring shoot-borne auxin[18]. On the contrary, other reports suggest that auxin promotes CSC differentiation[15,27]. Future studies will be necessary to clarify the nature of the HAN-dependent organizer signal.

Unique stemness-promoting factors exclusively expressed in stem cells have yet to be found, making this concept doubtful. As an alternative model, stemness might be defined by a combination of factors unique to stem cells, where each factor might also be expressed in other cells and have additional functions. In line with this, *HAN* expression is not limited to the root stem cell niche but has been implicated in several developmental processes[19,20]. Furthermore, although present in both cell types, the *WOX5/HAN/CDF4* cFFL directs *TAA1* expression only in the QC but not in CSCs, and HAN can completely replace the WOX5 function in CSC maintenance but only partially in the QC. Thus, the output of the *WOX5/HAN/CDF4* module depends on the cellular context, implying organizer and stem cell-specific cofactors.

HAN largely mimics the function of its upstream regulator, WOX5, in regulating endogenous CSCs and ectopic formation of iCSCs, including repressing the differentiation factor *CDF4*. Yet both activities do not act redundantly since a loss-of-function mutation in either gene results in CSC termination. So, what might be the biological role of the *WOX5/HAN/CDF4* module? The separate binding sites of WOX5 and HAN (**Fig. 5g**) suggest a non-competitive CDF4 inhibition, resulting in a NOR-gate logic of the cFFL module[30]. The NOR-gate cFFL module acts as a low-pass filter as it transduces slow varying signals, whereas fast changes are attenuated. This would dampen noisy signals into WOX5[31]. Further, the NOR-gate wiring results in a delayed response to a reduction of the input signal into the cFFL module (**Extended Data Fig. 8**). Altogether, the cFFL module with the NOR-gate has the potential to buffer the regulatory output against a transient reduction of WOX5 activity/concentrations, either stochastically or in response to a signal, and thus could function as a safeguard to block differentiation of CSCs against input noise. Future studies will address the dynamic range of this safeguard mechanism during stem cell homeostasis.

Acknowledgments

We are grateful to Dr. Hirokazu Tsukaya for sharing materials. We thank Sjon Hartman and members of the Laux lab for their comments on the manuscript. This work was funded by grants from the German Research Foundation (DFG) under Germany's Excellence Strategy (CIBSS - EXC-2189 - Project ID390939984), GRK2344, and La606/18 to T.L. CF received funding from an FET-Open research and innovation actions grant under the European Union’s Horizon 2020 (CyGenTiG; grant agreement 801041).

Methods:

Plant materials

This study used the *Arabidopsis* ecotype Columbia-0 (Col-0) as a wild-type background. The *wox5-1* mutant (and combinations with QC184 and QC25 markers) and *35S:WOX5-GR* inducible overexpression lines have been previously described[13,14]. The *han-30* and backcrossed *han-1* mutants were previously described and generously provided by Hirokazu Tsukaya, University of Tokyo[26]. For root microscopy, seeds were sown on ½ MS medium (2.15g/L Murashige & Skoog Medium including vitamins, Duchefa, Haarlem, The Netherlands), pH set to 5.7 with KOH and 10 g/L agar (Agar Agar SERVA High Gel Strength, SERVA, Heidelberg) and grown for six days in a Percival incubator at 18°C±2 under long-day conditions. *J2431* and *Q0680* have been established as part of the enhancer trap collection by J. Haseloff (http://haseloff.plantsci.cam.ac.uk/ and[32].

Fluorescence-activated cell sorting (FACS)

Seedlings containing the *35S:WOX5-GR* inducible overexpression construct and the *Q0680* marker were treated with either 5 µM dexamethasone or a mock solution. FACS was carried out at the Clinical Research Center of the University of Freiburg. RNA was extracted from GFP-positive protoplasts immediately following their collection.

Microarray data analysis and selection of candidate genes

Total RNA was isolated and verified for high quality with the Bioanalyzer 2100 (Agilent Technologies, Waldbronn, Germany). Following the manufacturer's instructions for the Quick-Amp and Hybridization kits (Agilent Technologies, Waldbronn Germany, part numbers 5190-2306 and 5188-5242, respectively), the RNA was labeled and hybridized to Agilent 4 x 44 k, Arabidopsis version 4, 2-colour microarrays (Agilent Technologies, Waldbronn Germany, part

number G2519F). RNA of dexamethasone-treated *35S:WOX5-GR; Q0680* was hybridized against that of dexamethasone-treated C24. As a control, the RNA of mock-treated *35S:WOX5-GR; Q0680* was hybridized against that of mock-treated C24. Immediately after drying, the microarrays were scanned on a G2565BA array scanner (Agilent Technologies, Waldbronn Germany), and intensities were recorded using the provided Feature Extraction software. Raw foreground and background intensities were analyzed in R version 2.15.1 (http://www.r-project.org) using packages from the Bioconductor version 2.18.0 project (Gentleman et al., 2004). Normalization of intensities and differential expression of genes was determined with the limma version 3.14.4 package (Smyth et al., 2005) using at least three biological replicates. The same package was also used to output the overlap of gene lists (at log2-fold change ≥ 1 and adjusted p-value ≤ 0.05 cutoffs). Data mining was done on the lists using the FileMaker Pro software (FileMaker Inc., version 10. 0). List of genes differentially regulated after 1h and 4h of *35S:WOX5-GR* induction by DEX are shown in the supplementary Table 1-3.

RT-qPCR

RT-qPCR experiment was used to assess the relative expression of genes. Five-day-old ½ MS grown seedlings were treated with liquid ½ MS media containing (10 µM) DEX for 15 min by flooding, and then plants were kept vertically for 4h. ½ MS plates supplemented with an equal volume of EtOH (EtOH volume used for DEX) were used as mock controls. Approximately 4-5 mm of root tissues were cut and harvested. Total plant RNA was isolated using Qiagen RNeasy Plant Mini Kit. 2 µg of RNA was used to prepare the complementary DNA (cDNA). cDNA was prepared using the PrimeScript 1st strand cDNA Synthesis Kit by Takara. 1:10 dilution of cDNA was used to test the relative expression between different genotypes. RT-qPCR was performed using the Sybr Green reagent from Applied Biosystems. Gene expression values were calculated as ΔΔCt. AT1G13440 (GACP2) and 18S rRNA were used as reference

353 genes to calculate relative expression values (2ΔCt values). All primers used are mentioned in
354 Table S4.
355
356 **Microscopy**
357 Nomarski microscopy (Differential Interference Contrast - DIC) was used to study root
358 morphology or GUS stainings. For visualization of starch granules, roots were shortly exposed
359 to Lugol solution (Sigma) and subsequently cleared in chloral hydrate solution (w/w: chloral
360 hydrate 80g, H_2O 30g, glycerine 10g gently mixed for 24 hours and stored at 4°C) on the
361 microscope slide. A Zeiss "Axioskop 2 plus" microscope was used to observe the resulting
362 microscope slides.
363 For confocal imaging of fluorescent markers, cell walls were stained by mounting roots in 10
364 µg/ml propidium iodide solution (Sigma). Confocal microscopy was performed using a
365 confocal laser scanning microscope LSM700 (Zeiss). Images were captured using LSM
366 software ZEN 2010 (Zeiss). For the detection of DsRed signals, roots were not stained with
367 propidium iodide, and DIC channel images were recorded to visualize the root with the DsRed
368 signal.
369 For mPS-PI staining, roots were fixed under vacuum for 1-2 min (fixative: 50% methanol, 10%
370 acetic acid, and 40% H_2O) and washed with water. Following fixation, roots were treated with
371 1% periodic acid with mild shaking for 15 min and then washed with water. After incubation
372 with periodic acid, the roots were first subjected to pseudo Schiff's solution (100 mM sodium
373 metabisulfite and 0.15 N HCl). Then, a freshly prepared PI solution (10 mg/mL) was added.
374 When the roots appeared colored pink, placed them in chloral hydrate and imaged immediately.
375
376 YFP-signal strength inside the QC nuclei was measured to quantify fluorescence intensities
377 using FIJI image analysis software (https://fiji.sc). Intensity values of two QC nuclei were

averaged to obtain one value for each root examined. Since the roots contained the *pWOX5:erCFP* reporter to visualize the QC cells, CFP and YFP channels were recorded separately to avoid interfering with YFP intensity measurements. The significance of the measured values was tested using InStat3 software (GraphPad Software).

Dexamethasone (DEX) treatments

For induction of transgenes by DEX treatments, seedlings were either germinated on or transferred to ½ MS plates supplemented with DEX (stock dissolved in EtOH) at the appropriate time before the experiment. In addition, ½ MS plates supplemented with EtOH were used as mock controls.

Chromatin immunoprecipitation (ChIP)

ChIP assays were performed as previously described (Saleh et al., 2008) with minor modifications. Briefly, five-day-old Col-0, *35S:LhGR pOp:WOX5-3xFlag* and *35S:Gal4-VP16-GR; UAS:3xFLAG-HAN-CDS* plants were treated with DEX (10 µM) for 15 min by flooding, and then plants were kept vertically for 4h or 6h, respectively. Approximately 4-5 mm of root tissues were cut and crosslinked with 1% formaldehyde, followed by ChIP and qPCR. For histone acetylation/methylation ChIP, root tissues were harvested without cross-linking. HAN-bound promoter fragments were enriched using anti-Flag antibodies (Sigma; F1804). For H3K9Ac and H3K27me3 ChIP, promoter fragments were enriched using Anti-acetyl-Histone H3 (Lys9) antibodies (07-352) and Anti-trimethyl-Histone H3 (Lys27) antibodies (07-449), respectively. Col-0 plants were taken as a negative background control. *ACTIN2 (ACT2)* and *GAPC2* promoter DNA were taken as negative controls.

Cloning of transgenes

Amplifying fragments for cloning was done using Phusion polymerase (NEB) according to the supplied protocol (for details on oligonucleotides used to amplify fragments for cloning, see Supplementary Table 4). Fragments were subcloned into pJET1.2 vector (Fermentas) according to the manufacturer's instructions and sequenced (GATC) to confirm the integrity of the sequence. Final constructs were assembled in pGreen-based plant transformation vectors harboring resistance genes for MTX or NORF (generously provided by Renze Heidstra). The *pHAN:NLS-3xYFP* reporter gene was constructed by ligation-independent cloning (LIC - adapted from[33,34].

References:

1 Aichinger, E., Kornet, N., Friedrich, T. & Laux, T. Plant stem cell niches. *Annu Rev Plant Biol* **63**, 615-636 (2012).

2 Laux, T. The stem cell concept in plants: a matter of debate. *Cell* **113**, 281-283 (2003).

3 Heidstra, R. & Sabatini, S. Plant and animal stem cells: similar yet different. *Nat Rev Mol Cell Biol* **15**, 301-312 (2014).

4 Clowes, F. A. L. The Cytogenerative Centre in Roots with Broad Columellas. *New Phytologist* **52**, 48-57 (1953).

5 Clowes, F. A. L. Localization of Nucleic Acid Synthesis in Root Meristems. *Journal of Experimental Botany* **7**, 307-& (1956).

6 van den Berg, C., Willemsen, V., Hendriks, G., Weisbeek, P. & Scheres, B. Short-range control of cell differentiation in the *Arabidopsis* root meristem. *Nature* **390**, 287-289 (1997).

7 Pardal, R. & Heidstra, R. Root stem cell niche networks: it's complexed! Insights from Arabidopsis. *Journal of Experimental Botany* **72**, 6727-6738 (2021).

8 Dubrovsky, J. G. & Ivanov, V. B. The quiescent centre of the root apical meristem: conceptual developments from Clowes to modern times. *Journal of Experimental Botany* **72**, 6687-6707 (2021).

9 Sakakibara, K. *et al.* WOX13-like genes are required for reprogramming of leaf and protoplast cells into stem cells in the moss Physcomitrella patens. *Development* **141**, 1660-1670 (2014).

10 Forzani, C. *et al.* WOX5 Suppresses *CYCLIN D* Activity to Establish Quiescence at the Center of the Root Stem Cell Niche. *Curr Biol* (2014).

11 Betegon-Putze, I. *et al.* Precise transcriptional control of cellular quiescence by BRAVO/WOX5 complex in Arabidopsis roots. *Mol Syst Biol* **17**, e9864 (2021).

12 Burkart, R. C. *et al.* PLETHORA-WOX5 interaction and subnuclear localization control Arabidopsis root stem cell maintenance. *EMBO Rep* **23**, e54105 (2022).

13 Sarkar, A. *et al.* Conserved factors regulate signalling in *Arabidopsis thaliana* shoot and root stem cell organizers. *Nature* **446**, 811-814 (2007).

14 Pi, L. *et al.* Organizer-Derived WOX5 Signal Maintains Root Columella Stem Cells through Chromatin-Mediated Repression of CDF4 Expression. *Dev Cell* **33**, 576-588 (2015).

15 Ding, Z. & Friml, J. Auxin regulates distal stem cell differentiation in Arabidopsis roots. *Proc Natl Acad Sci U S A* **107**, 12046-12051 (2010).

16 Sabatini, S. *et al.* An auxin-dependent distal organizer of pattern and polarity in the Arabidopsis root. *Cell* **99**, 463-472 (1999).

17 Blilou, I. *et al.* The PIN auxin efflux facilitator network controls growth and patterning in Arabidopsis roots. *Nature* **433**, 39-44 (2005).

18 Brumos, J. *et al.* Local Auxin Biosynthesis Is a Key Regulator of Plant Development. *Dev Cell* **47**, 306-318 e305 (2018).

19 Zhao, Y. *et al.* HANABA TARANU Is a GATA Transcription Factor That Regulates Shoot Apical Meristem and Flower Development in Arabidopsis. *Plant Cell* **16**, 2586-2600 (2004).

20 Nawy, T. *et al.* The GATA factor HANABA TARANU is required to position the proembryo boundary in the early Arabidopsis embryo. *Dev Cell* **19**, 103-113 (2010).

21 Berckmans, B., Kirschner, G., Gerlitz, N., Stadler, R. & Simon, R. CLE40 Signaling Regulates Root Stem Cell Fate. *Plant Physiol* **182**, 1776-1792 (2020).

22 Ricci, W. A. *et al.* Widespread long-range cis-regulatory elements in the maize genome. *Nat Plants* **5**, 1237-1249 (2019).

23 Lu, Z. *et al.* The prevalence, evolution and chromatin signatures of plant regulatory elements. *Nat Plants* **5**, 1250-1259 (2019).

24 Lin, Y., Zhao, H., Kotlarz, M. & Jiang, J. Enhancer-mediated reporter gene expression in Arabidopsis thaliana: a forward genetic screen. *Plant J* **106**, 661-671 (2021).

25 Zhang, Y. *et al.* Dynamic enhancer transcription associates with reprogramming of immune genes during pattern triggered immunity in Arabidopsis. *BMC Biol* **20**, 165 (2022).

26 Kanei, M., Horiguchi, G. & Tsukaya, H. Stable establishment of cotyledon identity during embryogenesis in Arabidopsis by ANGUSTIFOLIA3 and HANABA TARANU. *Development* **139**, 2436-2446 (2012).

27 Tian, H. *et al.* WOX5-IAA17 feedback circuit-mediated cellular auxin response is crucial for the patterning of root stem cell niches in Arabidopsis. *Mol Plant* **7**, 277-289 (2014).

28 Savina, M. S. *et al.* Cell Dynamics in WOX5-Overexpressing Root Tips: The Impact of Local Auxin Biosynthesis. *Front Plant Sci* **11**, 560169 (2020).

29 Stepanova, A. N. *et al.* TAA1-mediated auxin biosynthesis is essential for hormone crosstalk and plant development. *Cell* **133**, 177-191 (2008).

30 Mangan, S. & Alon, U. Structure and function of the feed-forward loop network motif. *Proc Natl Acad Sci U S A* **100**, 11980-11985 (2003).

31 Cortijo, S. & Locke, J. C. W. Does Gene Expression Noise Play a Functional Role in Plants? *Trends Plant Sci* **25**, 1041-1051 (2020).

32 Sabatini, S., Heidstra, R., Wildwater, M. & Scheres, B. SCARECROW is involved in positioning the stem cell niche in the Arabidopsis root meristem. *Genes Dev* **17**, 354-358 (2003).

33 De Rybel, B. *et al.* A versatile set of ligation-independent cloning vectors for functional studies in plants. *Plant Physiol* **156**, 1292-1299 (2011).

34 Eschenfeldt, W. H., Lucy, S., Millard, C. S., Joachimiak, A. & Mark, I. D. A family of LIC vectors for high-throughput cloning and purification of proteins. *Methods Mol Biol* **498**, 105-115 (2009).

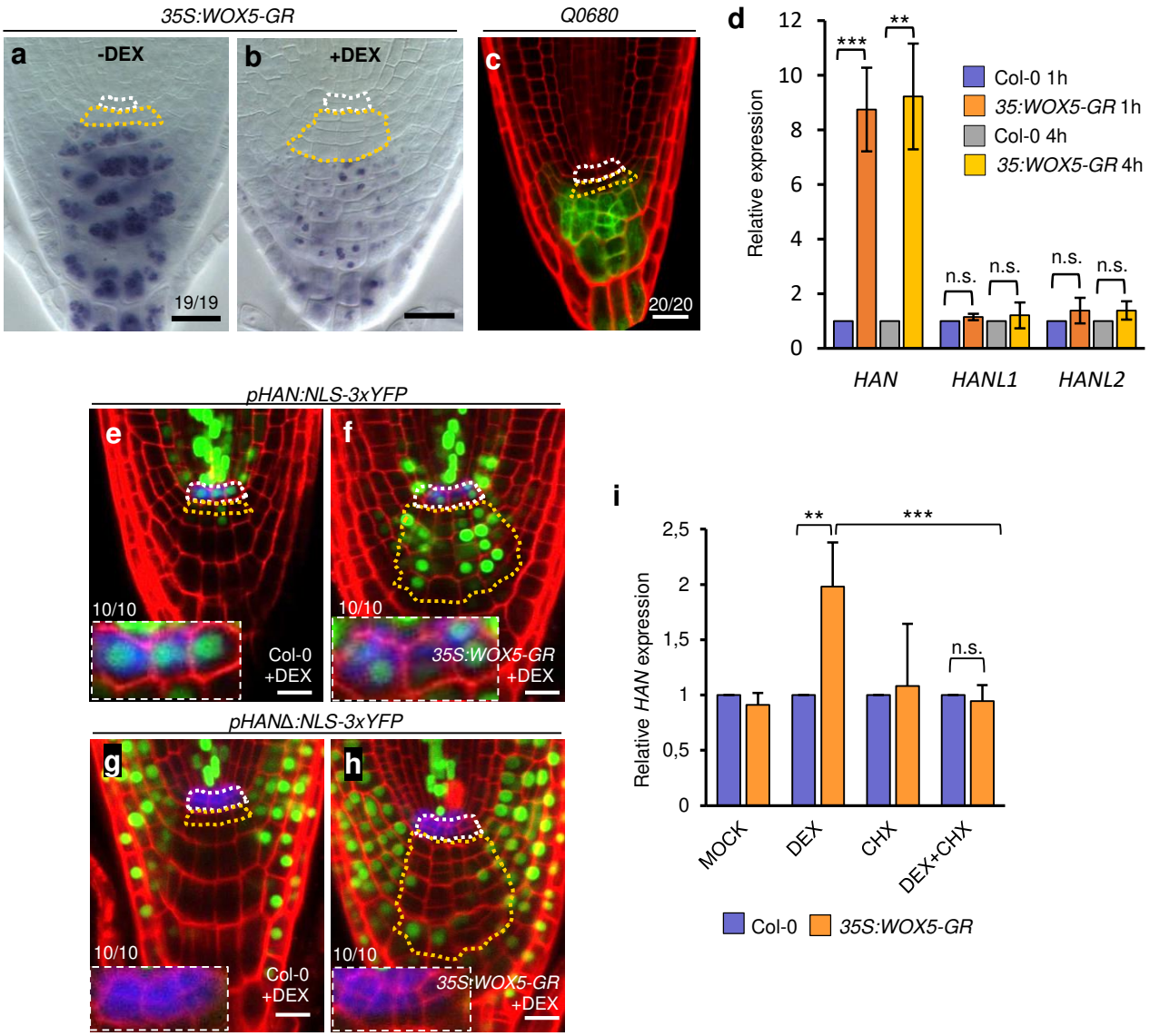

Fig. 1: Ectopic WOX5 activity in columella root cap cells upregulates *HAN* transcription

a-b: DIC images of root tips after Lugol staining of starch grains (blue). *35S:WOX5-GR* plants show a normal root tip morphology when uninduced (a) but trigger the formation of columella stem cell-like cells after DEX treatment (b).

c: *Q0680:erGFP* signal marks differentiated columella cells (CCs) and was used to isolate them by FACS.

d: Expression of *HAN* is strongly upregulated in sorted CCs 1 and 4h after DEX induction of *35S:WOX5-GR*, but *HAN-like (HANL)* genes remain unchanged. Data were normalized to DEX-treated Col-0 wild type. **, p <0.01; ***, p <0.001 by Student's *t*-test.

e-f: *pHAN:NLS-3xYFP* expression is upregulated in CCs after 24h DEX treatment of *35S:WOX5-GR* (f) compared to Col-0 wild type (e). QC cells are labeled by a *pWOX5:erCFP* marker (blue).

g-h: Expression of *pHANΔ530bp:NLS-3xYFP* (green) in Col-0 (g) and *35S:WOX5-GR* (h) after 24h DEX treatment.

i: RT-qPCR expression of *HAN* transcripts in Col-0 and *35S:WOX5-GR* after treatment with MOCK, DEX (10 µM), CHX (10 µM) and DEX+CHX (10 µM) for 4h. Data shown are means of three independent biological replicates. Error bars denote SD. n.s., not significant; **, p<0.01 by One-way ANOVA with Tukey's multiple comparison correction.

Confocal images (c, e-f, g-h) with cell walls stained with propidium iodide (red) and QC cells labeled by *pWOX5:erCFP* (blue, e-f, g-h). The QC (white) and the CSCs/iCSCs (yellow) are outlined.

y/x denote frequencies of observations.

Scale bars: 20µm.

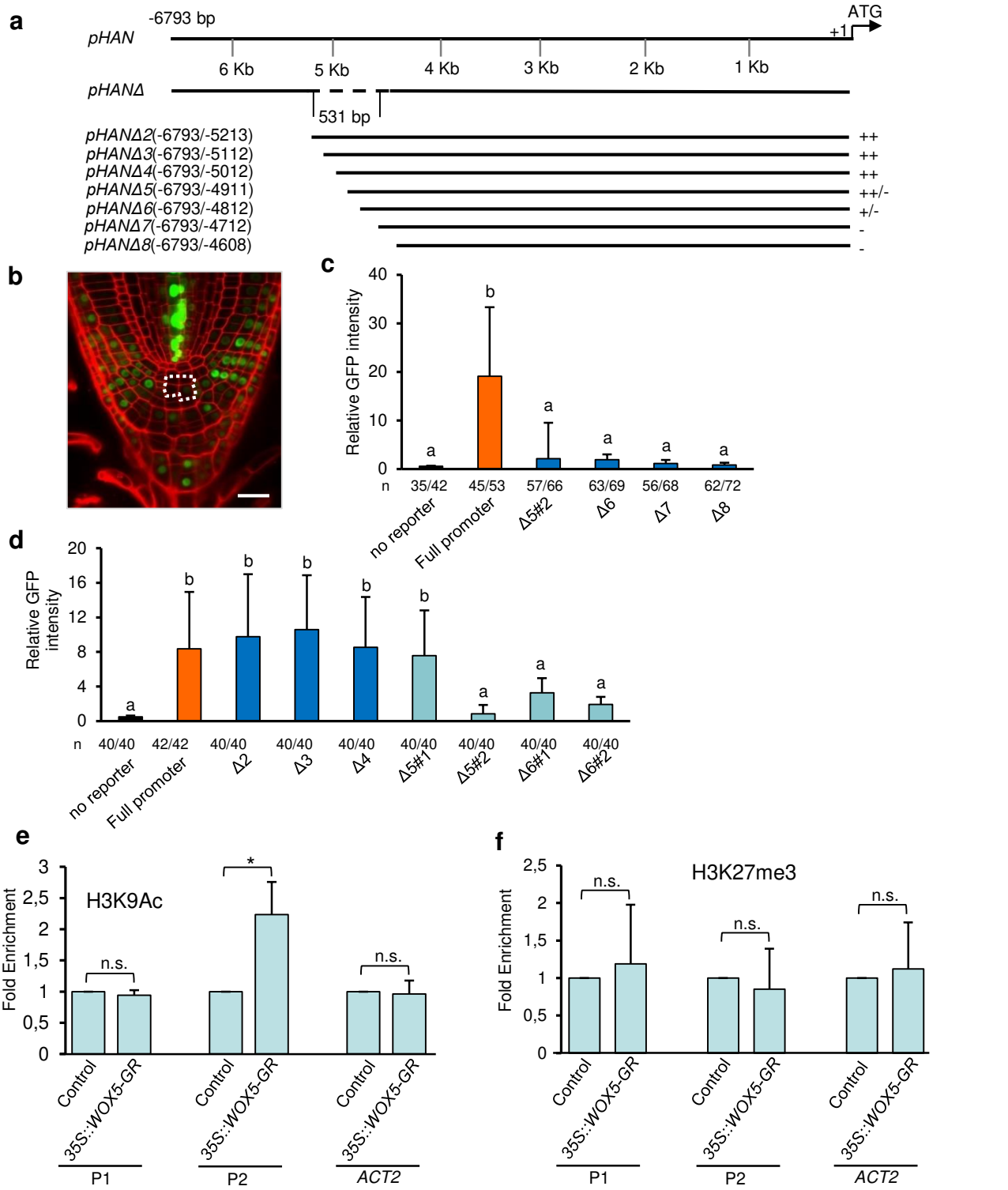

Extended Data Fig. 1: A distal regulatory element in the HAN promoter is required for activation by WOX5
a: Schematic representation of the *HAN* promoter and the corresponding deletion constructs. ++, inducible expression in CCs by *35S:WOX5-GR* similar to the complete *pHAN:3xGFP*, +, weakly inducible, - not inducible.
b: Outline of the central 4 CCs used for signal quantification.
c-d: Results of the two experiments comparing representative lines from *pΔ2HAN* to *pΔ6HAN* (d) and from *pΔ5HAN* to *pΔ8HAN* (c). Values show the relative increase in GFP signal measured after 24h of *35S:WOX5-GR* induction. WOX5-GR represents a negative control without GFP reporter. x/y, roots analyzed without (x) and with (y) DEX induction. Letters denote statistical differences at $p < 0.001$ compared to the "full promoter" by one-way ANOVA and Dunnett's posthoc test.
e-f: Induction of *35S:LhGR pOp:WOX5-3xFlag (35S::WOX5-GR)* line causes relative enrichment of H3K9Ac deposition on the distal regulatory element (*p2: 5021 bp upstream to ATG*) of the *HAN* gene relative to *Q1630::H2B-tdTomato* as negative control. By contrast, the P1 site (-654) and H3K27me3 marks were unaffected. The data shown are means of three independent biological replicates. Error bars denote SD. n.s., not significant; *, p<0.05 by Student's *t*-test.
Scale bar: 20μm

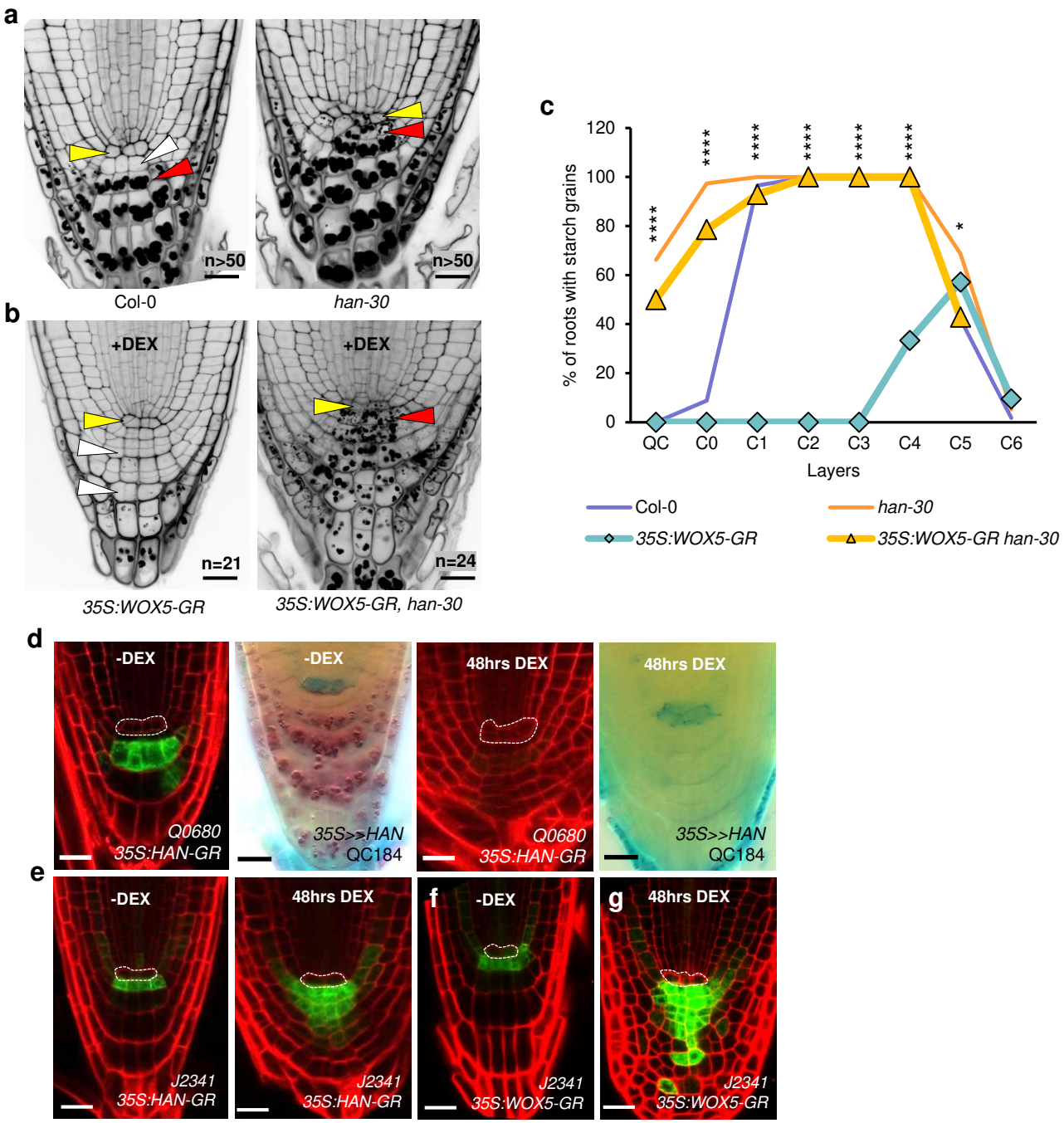

Fig. 2: HAN acts downstream of WOX5 during the induction of CSC-like cells

a-b: Representative confocal images of six-day-old roots showing accumulation of starch-positive amyloplasts in the indicated genotypes after 24 h of DEX treatment, followed by mPS-PI-staining. White arrowheads indicate the CSC layer, red arrowheads the starch grains in the differentiated cell layers, and yellow arrowheads the QC position.

c: Percentage of roots with starch grains in different layers of the indicated genotypes. *, $p<0.05$; ****, $p<0.0001$ by Fisher's exact test comparing *35S:WOX5-GR* and *35S:WOX5-GR han-30* genotypes.

d: Induction of HAN expression after DEX treatment as indicated. Left images, confocal images of PI-stained *35S:HAN-GR* expressing roots carrying the CC reporter *QC0680:erGFP*. Right images, DIC images of roots expressing *35S:Gal4-VP16-GR UAS:HAN* (*35>>HAN*). Lugol staining shows starch grains in the CCs (brown) and blue signal shows expression of the QC-specific reporter QC184:GUS.

e-g: Expression of the columella stem cell marker J2341 (green) increases after induction of *35S:HAN-GR* (e), similarly to after *35S:WOX5-GR* induction (f,g).

Representative images of n>20 roots from each of three independent lines (d-g). Scale bars: 20µm

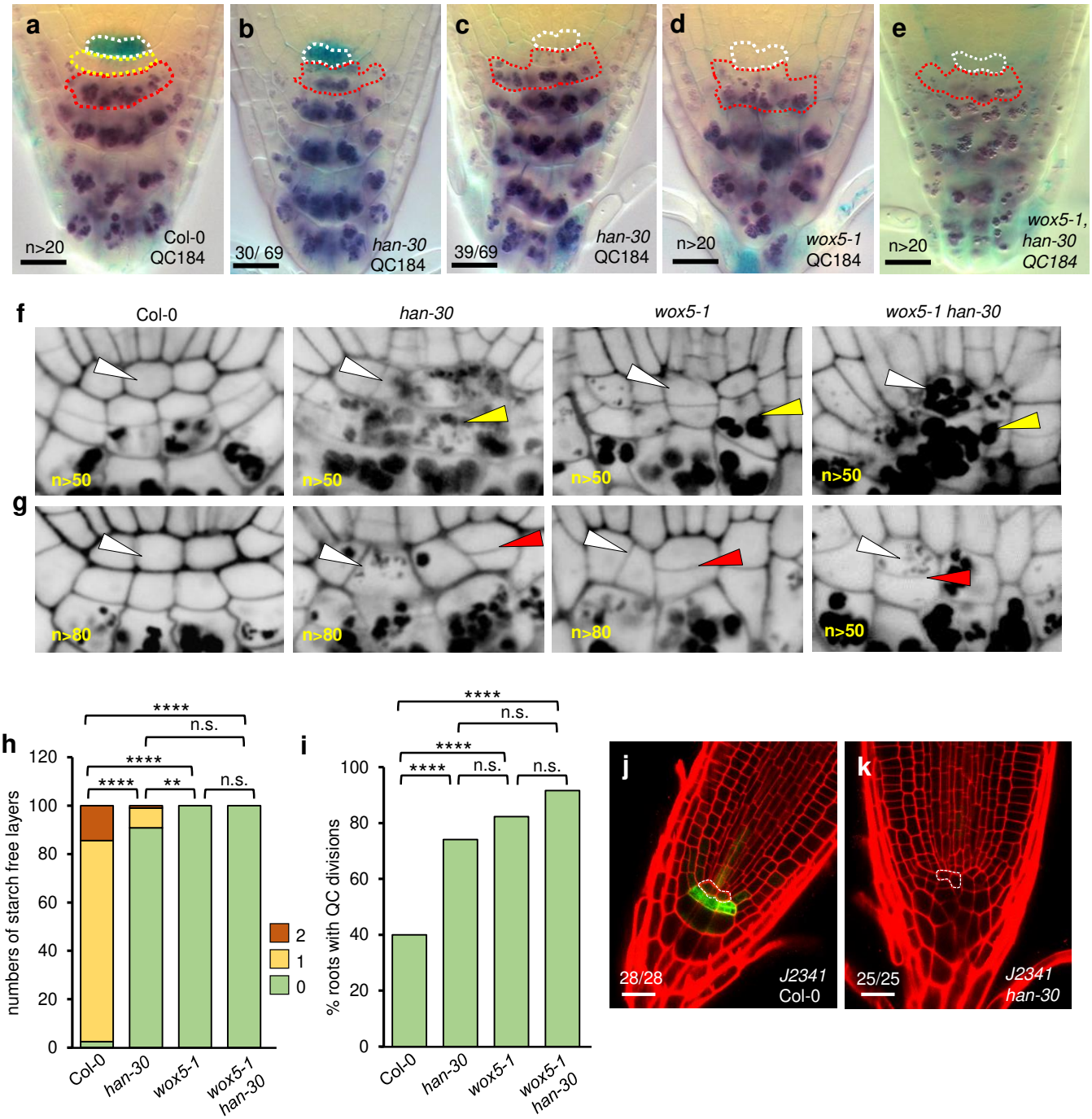

Fig. 3: HAN is required for QC and CSC identity in the columella stem cell niche

a-e: Representative DIC images of root tips of the indicated genotypes. QC184 signal after GUS staining is shown in blue and starch granules labeled by lugol staining in purple. Dotted lines mark QC cells (white), columella stem cells (yellow), and upper layers of differentiated CCs (red).

f: Representative confocal images showing ectopic starch grains at the CSC position (yellow arrowheads) of the indicated genotypes after mPS-PI-staining of the six-day-old roots. The position of the QC is indicated (white arrowheads).

g: Representative confocal images showing cell walls indicative of QC divisions (red arrowheads) of the indicated genotypes after mPS-PI-staining of the six-day-old roots. The position of the QC is indicated (white arrowheads).

h: Percentages of roots with different numbers of starch-free layers below the QC in six-day-old WT (n=83), *han-30* (n=110), *wox5-1* (n=105), and *wox5-1 han-30* (n=51) roots. n.s., not significant; **, $p<0.01$; ****, $p<0.0001$ comparing presence vs. absence of starch-free CSC layers by Fisher's exact test with Bonferroni correction for multiple testing.

i: Percentages of QC division in six-day-old WT (n=80), *han-30* (n=89), *wox5-1* (n=96), and *wox5-1 han-30* (n=48) roots. n.s., not significant; ****, $p<0.0001$ by Fisher's exact test with Bonferroni correction for multiple testing.

j-k: Representative confocal images showing expression of the CSC marker *J2341:GFP* in WT (j) and *han-30* (k). Scale bars: 20µm

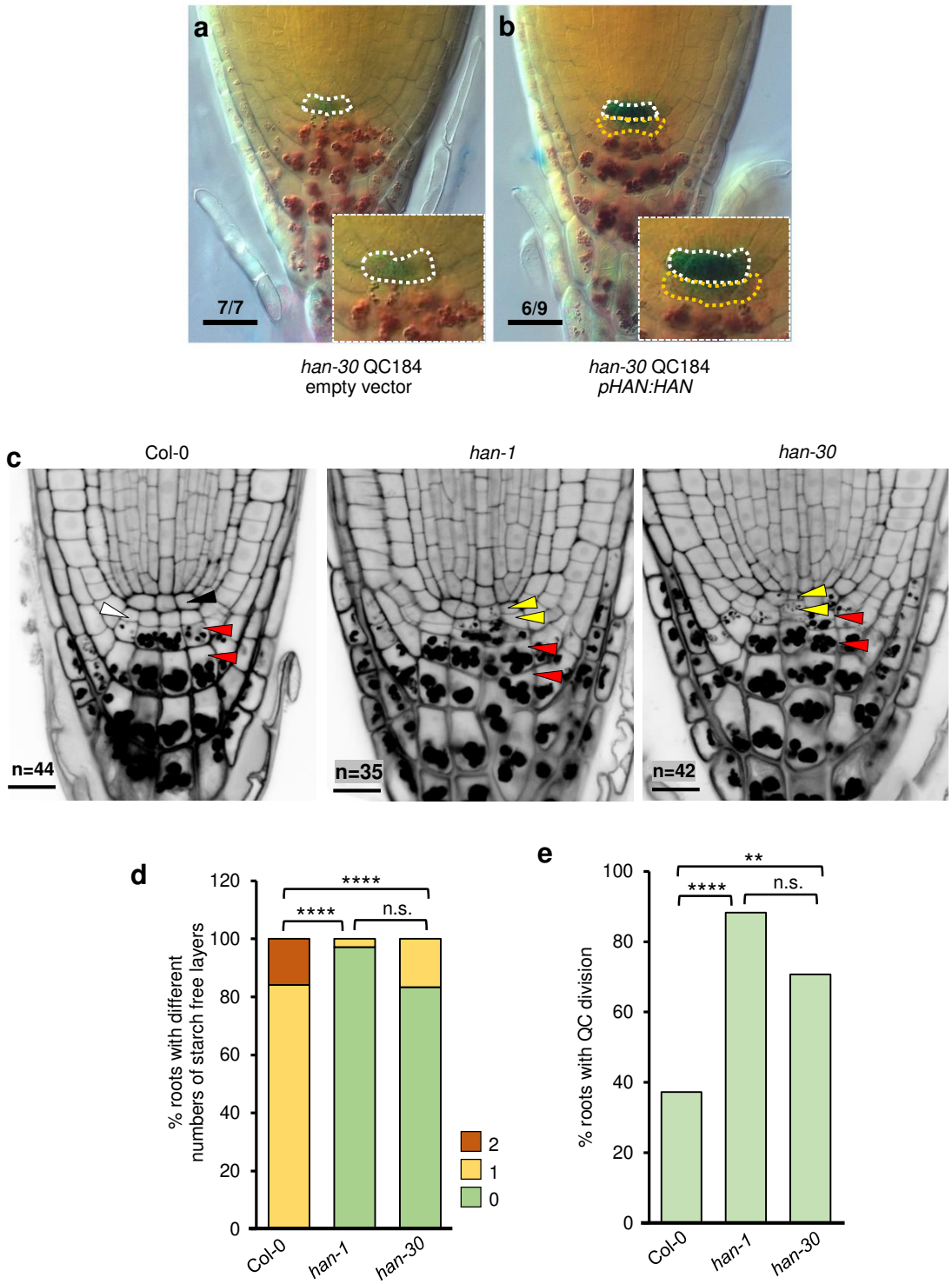

Extended Data Fig. 2: The *han-30* mutant is rescued by *pHAN:HAN* and displays similar CSC defects as the null allele *han-1.*

a-b: The reduced expression of QC184 and the accumulation of starch grains in the subjacent cell layer of 5-day-old *han-30* roots (a) are complemented by *pHAN:HAN* (b). Numbers denote the frequencies of the shown phenotypes in independent transformants. The QC is outlined in white. The restored CSCs are outlined in yellow (b).

c: Representative confocal images showing accumulation of starch-positive amyloplasts (red arrowheads) and QC divisions (yellow arrowheads) of the indicated genotypes after mPS-PI-staining of six-day-old roots. White arrowhead shows the CSC layer and black arrowhead shows the QC position in the wild type.

d: Percentage of roots with indicated numbers of starch-free CSC-like layers in six-day-old Col-0 wild type (n=44), *han-1* (n=34), and *han-30* (n=42) roots. n.s., not significant; ****, $p<0.0001$, comparing presence vs. absence of starch-free CSC layers by Fisher's exact test with Bonferroni correction for multiple testing.

e: Quantification of QC division in six-day-old Col-0 wild-type (n=43), *han-1* (n=34) and *han-30* (n=41) roots. n.s., not significant; **, $p<0.01$, ****, $p<0.0001$ by Fisher's exact test with Bonferroni correction for multiple testing.

Scale bars: 20µm

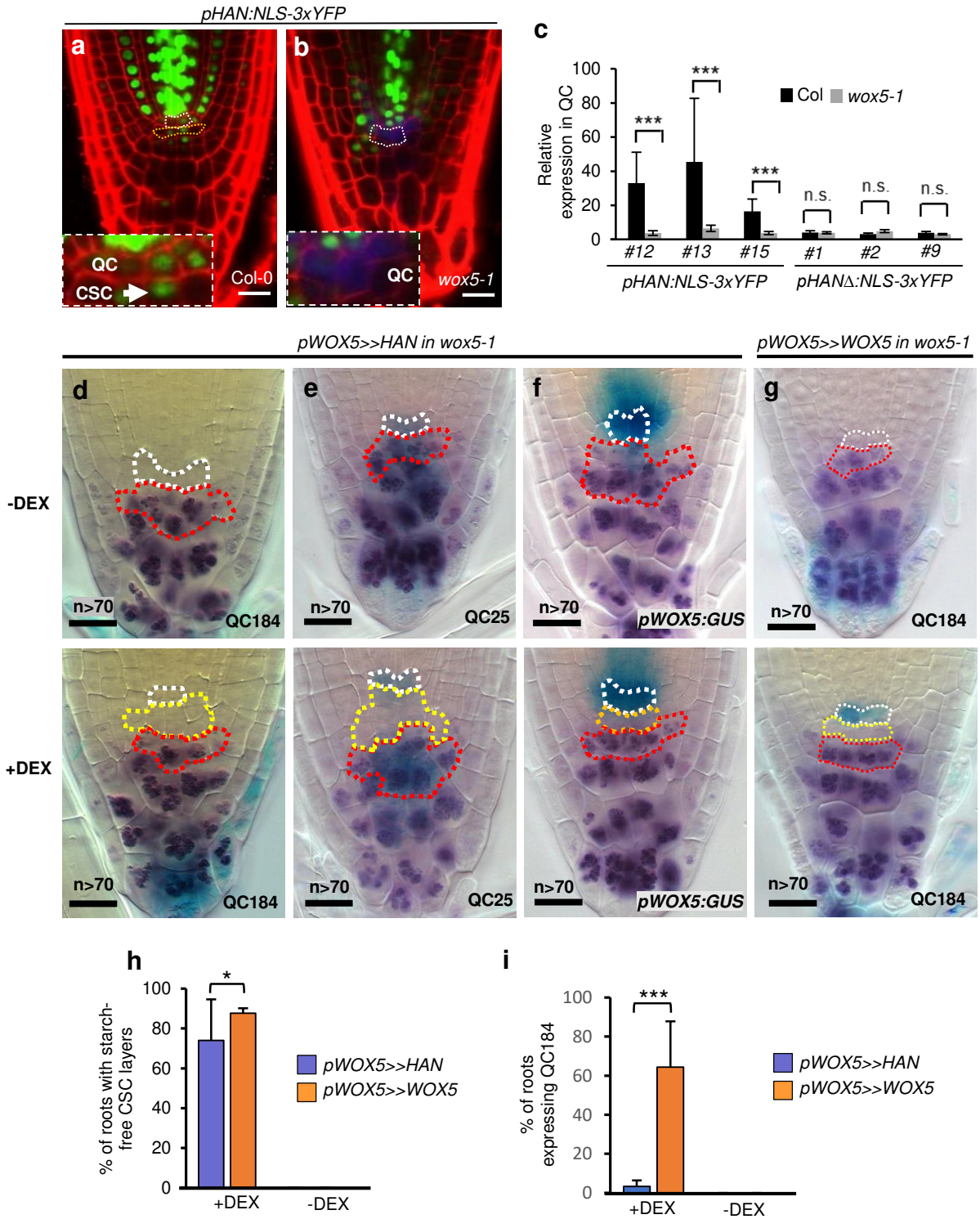

Fig. 4: Expression of HAN in the QC restores the CSC stemness but not expression of Q184 in *wox5-1* mutants

a-b: Representative images of *pHAN:NLS-3xYFP* expression in six-day-old roots of the indicated genotypes. Insets show magnifications of QC/CSC areas. *pWOX5:erCFP* signal (blue) marks the QC region in *wox5-1* (b).

c: Average YFP intensities in QC cells of three independent transgenic lines expressing *pHAN:NLS-3xYFP* or *pHANΔ:NLS-3xYFP* in Col-0 (black) or *wox5-1* (grey). Averages of at least 10 measurements are shown and normalized to background levels. Error bars denote SD. n.s., not significant; ***, $p< 0.001$ by Student's *t*-test.

d-f: *pWOX5>>HAN* induction in the indicated genotypes. -DEX, mock treated; +DEX, germination on 5 µM DEX for six days. Reporter gene signals are shown in blue and starch granules in purple. Dotted lines mark the QC cells (white), the CSCs (yellow), and the upper-layer CCs (red).

g: *pWOX5>>WOX5* results in a similar restoration of the stem cell niche in *wox5-1* as *pWOX5>>HAN,* but also re-established QC184 expression.

h-i: Percentages of the rescue of starch-free CSCs (h) and QC184 expression (i) in *wox5-1* by DEX-induction of *pWOX5>>HAN* and *pWOX5>>WOX5*. Bars indicate the mean values of at least 3 independent homozygous transgenic lines (n>70). Error bars denote SD. *, $p< 0.05$; ***, $p< 0.001$ by Fisher's exact test.

Scale bars: 20µm

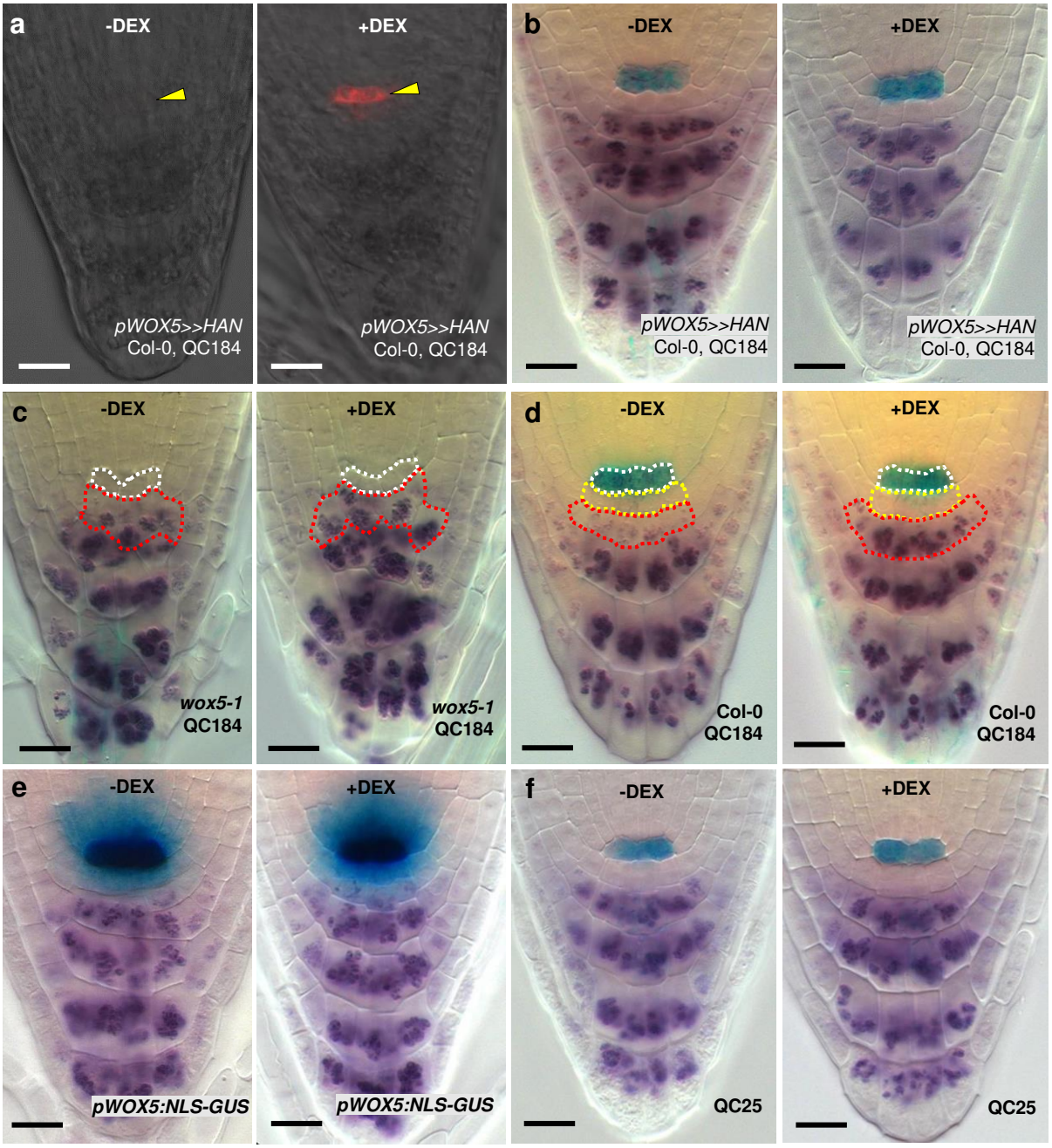

Extended Data Fig. 3: Dexamethasone itself does not affect the expression of QC markers

a: *pWOX5>>HAN* expression in Col-0 QC184 after DEX induction. Confocal images showing erDsRed expression in mock-treated roots and after germination on 5 µM DEX for six days (a). Yellow arrowheads indicate QC position.

b: Col-0 QC184 roots are unaffected by the induction of *pWOX5>>HAN*.

c-d: QC184 expression is not affected by germination on 5 µM DEX-containing medium for six days in the indicated genotypes.

e-f: *pWOX5:NLS-GUS* (e) and QC25 (f) expression is not affected by germination on 5 µM DEX-containing medium.

GUS signals (b-f) are shown in blue, and starch granules after Lugol staining in purple.

Representative images of n>20. Scale bars: 20µm

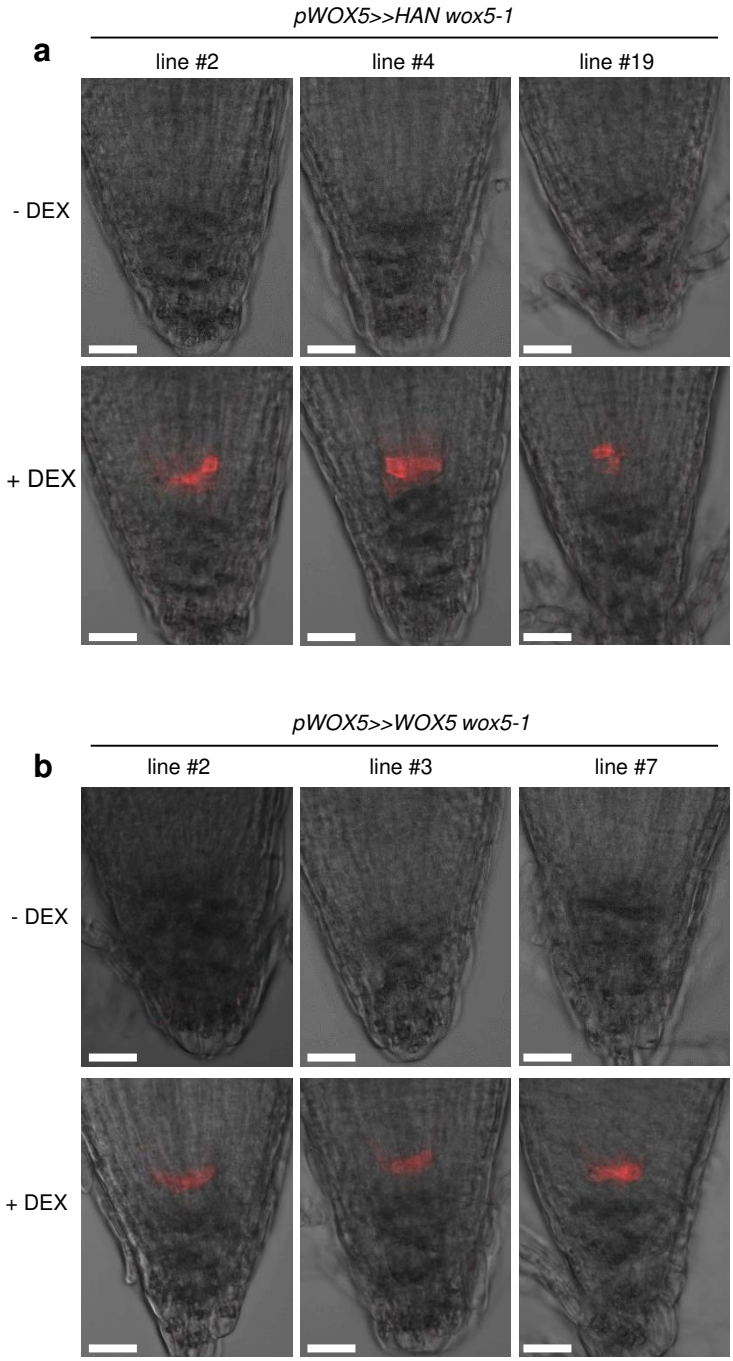

Extended Data Fig. 4: DEX application causes similar expression levels of *pWOX5>>HAN* and *pWOX5>>WOX5*

a: Expression of *pWOX5>>HAN* in three independent transformants in the *wox5-1* background.
b: Expression of *pWOX5>>WOX5* in three independent transformants in the *wox5-1* background.
-DEX, mock treated; +DEX, grown for six days after germination on 5 µM DEX.
DsRED signals and red color was equally enhanced for better visualization. Representative images of n>20. Scale bars: 25µm.

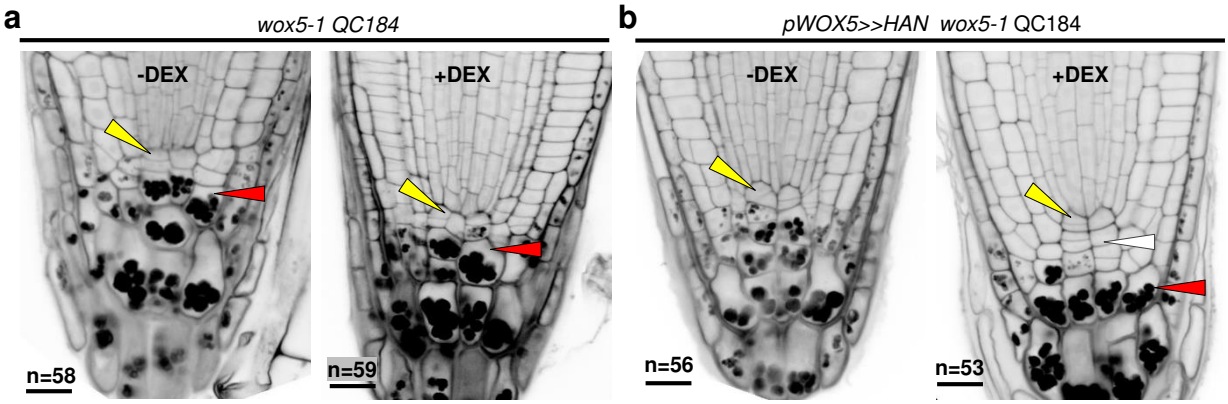

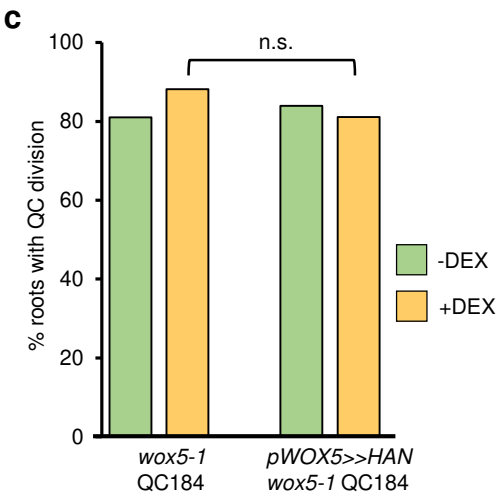

Extended Data Fig. 5: HAN expression in the QC does not suppress abnormal QC divisions in *wox5-1.*
a-b: Representative confocal images showing accumulation of starch-positive amyloplasts (red arrowheads) and QC divisions (yellow arrowheads) of the indicated genotypes after mPS-PI-staining of six-day-old roots. -DEX, mock treated; +DEX, grown for six days after germination on 10 µM DEX.
c: Percentage of roots with QC division in the indicated genotypes. n.s., not significant by Fisher's exact test.
Scale bars: 20µm

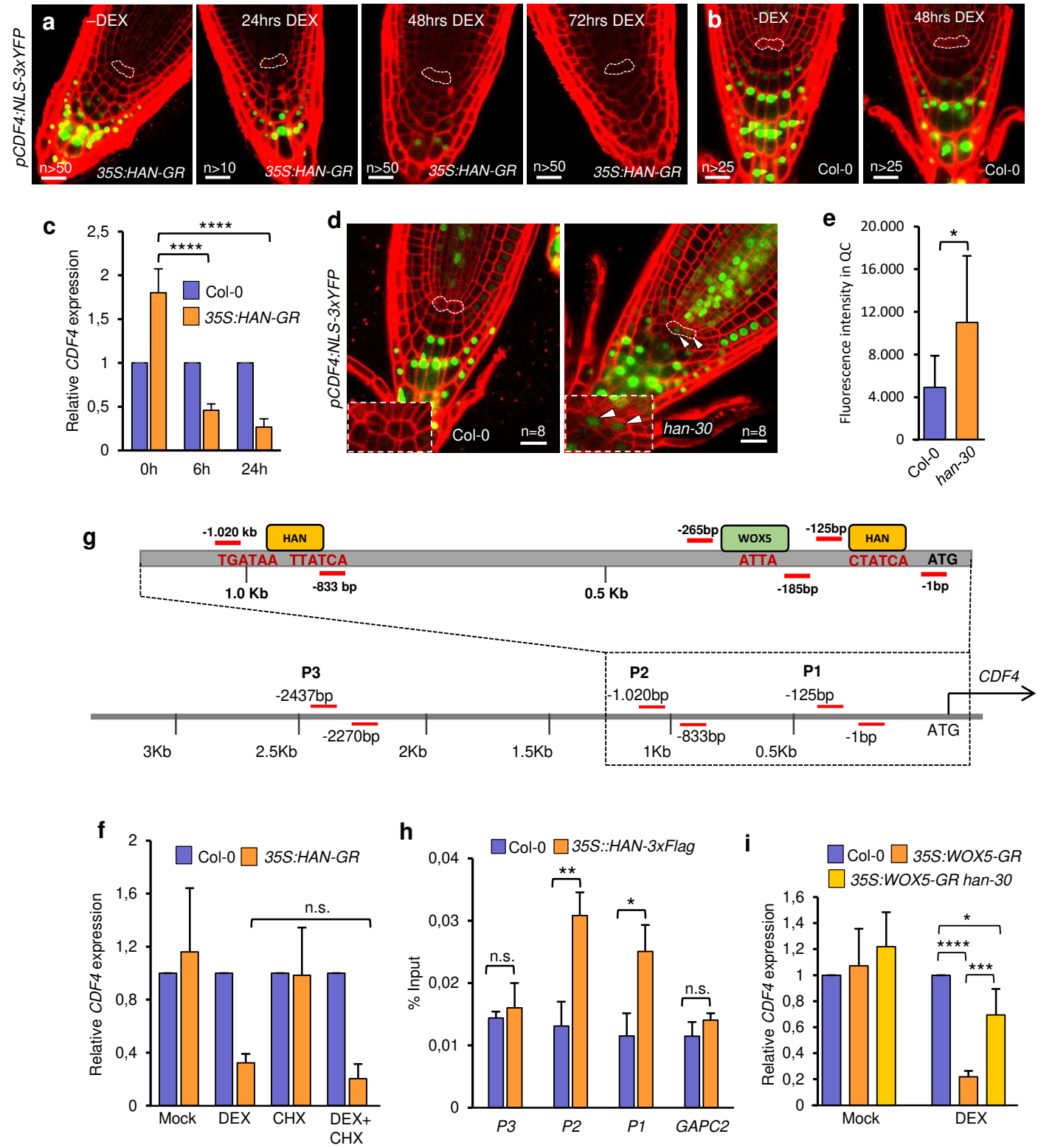
a
pCDF4:NLS-3xYFP
–DEX
24hrs DEX
48hrs DEX
72hrs DEX
n>50
35S:HAN-GR
n>10
b
-DEX
48hrs DEX
n>25
Col-0
c
Relative CDF4 expression
2,5
2
1,5
1
0,5
0
****
Col-0
35S:HAN-GR
0h
6h
24h
d
pCDF4:NLS-3xYFP
Col-0
n=8
han-30
e
Fluorescence intensity in QC
20.000
16.000
12.000
8.000
4.000
0
*
Col-0
han-30
g
-1.020 kb
HAN
TGATAA
TTATCA
1.0 Kb
-833 bp
-265bp
WOX5
ATTA
-125bp
HAN
CTATCA
ATG
0.5 Kb
-185bp
-1bp
P3
-2437bp
-2270bp
P2
-1.020bp
-833bp
P1
-125bp
-1bp
CDF4
ATG
3Kb
2.5Kb
2Kb
1.5Kb
1Kb
0.5Kb
f
Relative CDF4 expression
2
1,6
1,2
0,8
0,4
0
Col-0
35S:HAN-GR
n.s.
Mock
DEX
CHX
DEX+ CHX
h
% Input
0,04
0,03
0,02
0,01
0
Col-0
35S::HAN-3xFlag
**
*
n.s.
n.s.
P3
P2
P1
GAPC2
i
Relative CDF4 expression
1,6
1,4
1,2
1
0,8
0,6
0,4
0,2
0
Col-0
35S:WOX5-GR
35S:WOX5-GR han-30
*
****
***
Mock
DEX

Fig. 5: HAN directly represses *CDF4* transcription

a-b: DEX-induction of *35S:HAN-GR* causes repression of the *pCDF4:NLS-3xYFP* reporter in the CCs (a), whereas DEX alone did has no effect (b). Representative images of the indicated genotypes from three independent biological replicates.

c: Relative expression of *CDF4* in Col-0 and *35S:HAN-GR* after induction with DEX at the indicated time points. Data shown are the means of five independent biological replicates. Error bars denote SD. ****, p<0.0001 by One-way ANOVA with Dunnett's multiple comparisons test.

d: Representative confocal images showing expression of *pCDF4:NLS-3xYFP* in Col-0 wild-type and *han-30* background. Dotted white lines indicate QC.

e: Quantification of GFP intensity in two central QC cells of each genotype. The data shown are means of 8 roots of each genotype. *, *p*<0,05, Student's *t*-test.

f: RT-qPCR expression of *CDF4* in Col-0 wild type and *35S:HAN-GR* after treatment with MOCK, DEX (10 µM), CHX (10 µM) and DEX+CHX (10 µM) for 4h. Data shown are means of four independent biological replicates. Error bars denote SD. n.s., not significant; by Student's *t*-test.

g-h: ChIP analysis. The diagram in (**g**) shows the 3kb long promoter region of *CDF4* upstream of the ATG and positions of the ChIP-PCR primers. Magnification depicts 1 kb of the *CDF4* promoter containing the predicted GATA-binding motifs for HAN, and the WOX5 binding site (Pi et al 2015) for comparison. (**h**) shows specific HAN-3xFlag enrichment as % input at the *P1 and P2* sites upon 6h DEX induction (10 µM) of *35S:Gal4-VP16-GR; UAS:3xFLAG-HAN* and the Col-0 wild type. GAPC2 is taken as a negative control. The data are means of three independent biological replicates. Error bars denote SD. n.s., not significant; *, *p*<0.05; **, *p*<0.01; by Student's *t*-test.

i: RT-qPCR expression of *CDF4* in the Col-0 wild-type, *35S:WOX5-GR* and *35S:WOX5-GR han-30 roots* after treatment with DEX for 4h. Data shown are means of four independent biological replicates. Error bars denote SD. ****, *p*<0.0001, ***, *p*<0.001, *, *p*<0.05 by One-way ANOVA with Tukey's multiple comparisons test.

Scale bars: 20µm

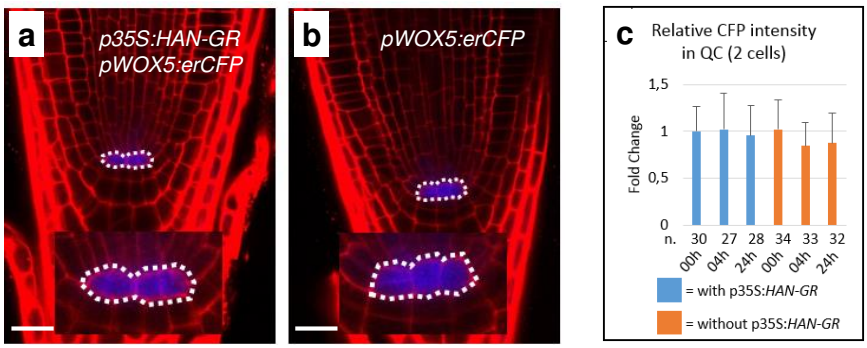

Extended Data Fig. 6: Ectopic *HAN* expression in the columella does not upregulate *pWOX5:erCFP* expression

a-b: Representative confocal images of *pWOX5:erCFP 35S:HAN-GR* (a) and *pWOX5:erCFP* (b) after 24h of DEX induction. Insets show magnifications of QC, marked by dotted lines.

c: Quantification of the CFP intensity measured in the two central QC cells; normalized to 0h. n, numbers of roots analyzed. Differences were not significant by Student's *t*-test between the two genotypes at each timepoint.

Scale bars: 20 µm

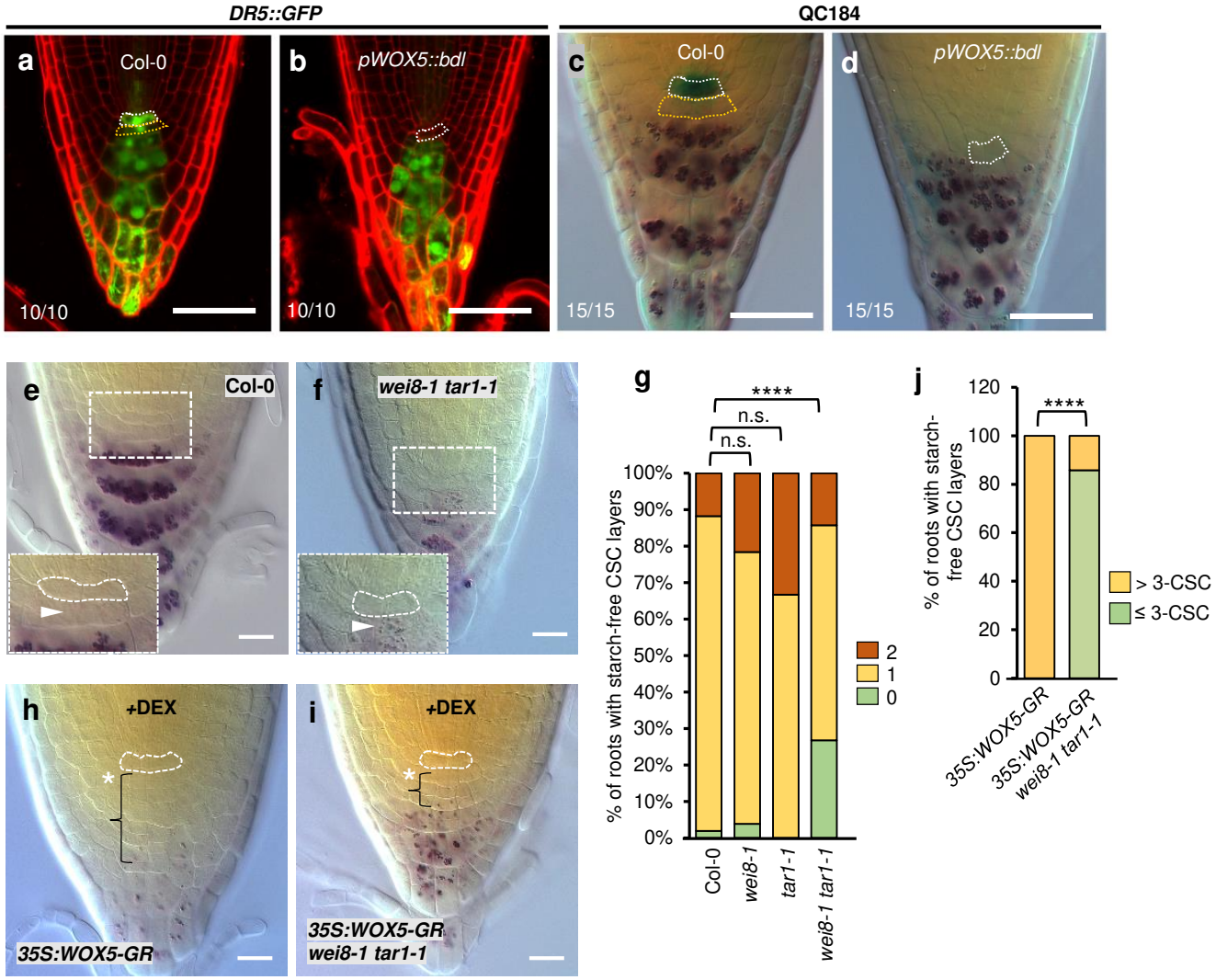

Extended Data Fig. 7: Auxin response and biosynthesis is required for CSC maintenance and iCSC induction by WOX5

a–b: *DR5:GFP* expression in the Col-0 wild type (a) and *pWOX5>>bdl* (b).

c-d: QC184 expression in the Col-0 wild type (c) and *pWOX5>>bdl* (d). In **a-d**, Representative images of root tips from at least 15 five-day-old seedlings per genotype. The QC (white) and the CSCs (yellow) are indicated. Scale bars: 50 µm.

e-f: Lugol-stained roots of the indicated genotypes in five-day-old seedlings. Termination of CSCs is indicated by the accumulation of starch granules in *wei8-1 tar1-1* mutants (f) compared to the Col-0 wild type (e). Insets show the magnification of CSC niche as indicated by white rectangular. The QC is outlined by dashed lines. White arrowheads indicate the CSC position.

g: Frequency of roots with indicated numbers of CSC layers in the indicated genotypes (n > 50 each genotype). n.s., not significant; ****, p<0.0001, comparing presence vs. absence of starch-free CSC layers by Fisher's exact test with Bonferroni correction for multiple testing.

h-i: iCSC induction by *WOX5* is largely suppressed in *wei8-1 tar1-1* (i), compared with *35S:WOX5-GR* in the Col-0 wild-type (h) background. Five-day-old seedlings were induced by 10 µM DEX for 16h. Dotted white lines indicate QC position. Asterisk with waved brackets indicate iCSC layers. **In e-i,** Scale bars: 20 µm

j: Quantification of the suppression of extra CSC layers as shown in (h-i). Error bars denote SD of 15 measurements. ****, p <0.0001 by Fisher's exact test.

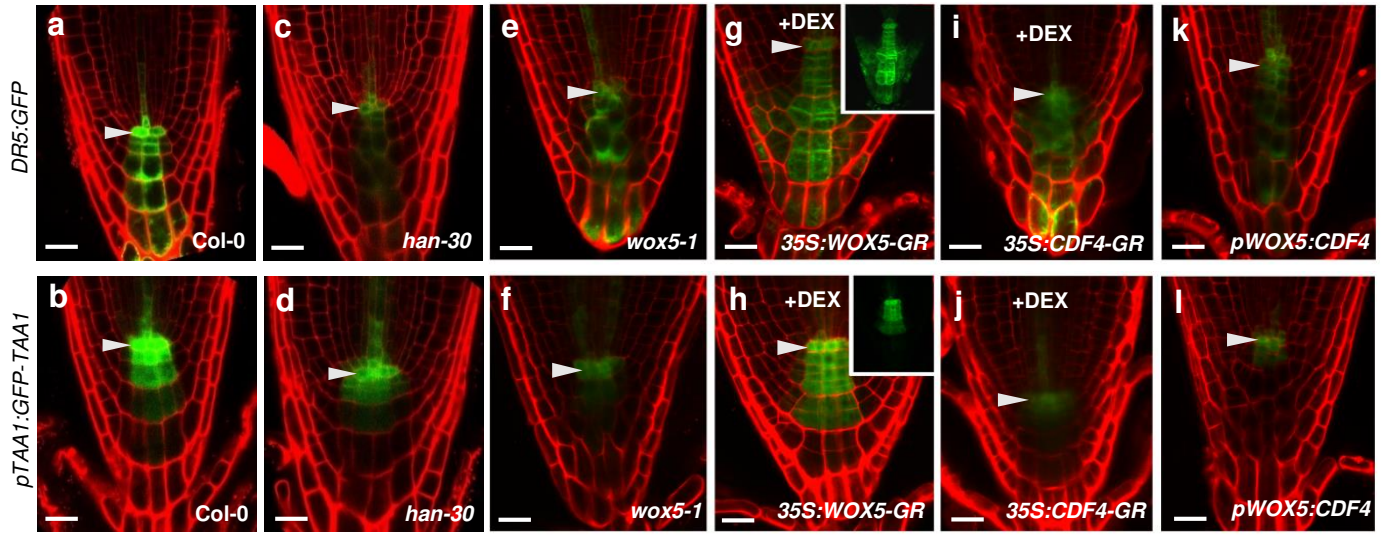
DR5:GFP
pTAA1:GFP-TAA1
a
b
Col-0
c
d
han-30
e
f
wox5-1
g
h
+DEX
35S:WOX5-GR
i
j
35S:CDF4-GR
k
l
pWOX5:CDF4

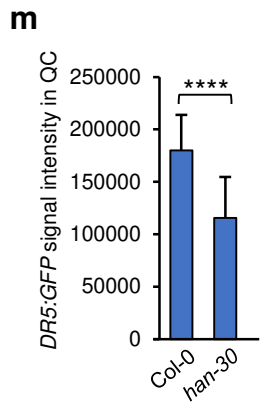
m
DR5:GFP signal intensity in QC
250000
200000
150000
100000
50000
0
****
Col-0
han-30

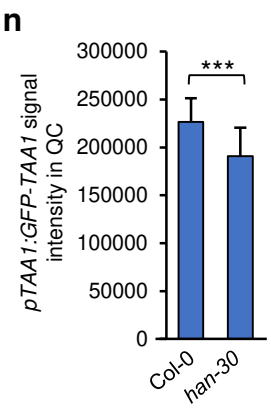
n
pTAA1:GFP-TAA1 signal intensity in QC
300000
250000
200000
150000
100000
50000
0
***
Col-0
han-30

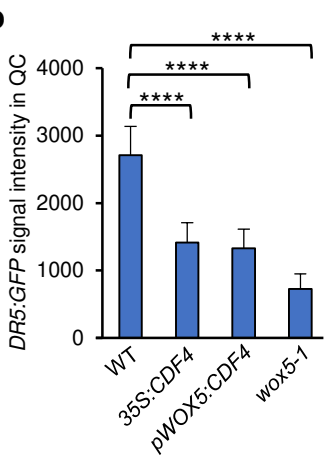
o
DR5:GFP signal intensity in QC
4000
3000
2000
1000
0
****
****
****
WT
35S:CDF4
pWOX5:CDF4
wox5-1

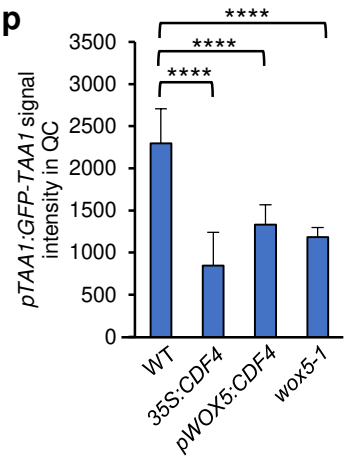
p
pTAA1:GFP-TAA1 signal intensity in QC
3500
3000
2500
2000
1500
1000
500
0
****
****
****
WT
35S:CDF4
pWOX5:CDF4
wox5-1

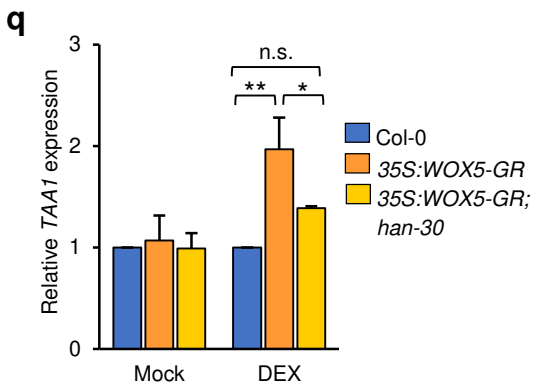
q
Relative TAA1 expression
3
2
1
0
n.s.
**
*
Col-0
35S:WOX5-GR
35S:WOX5-GR; han-30
Mock
DEX

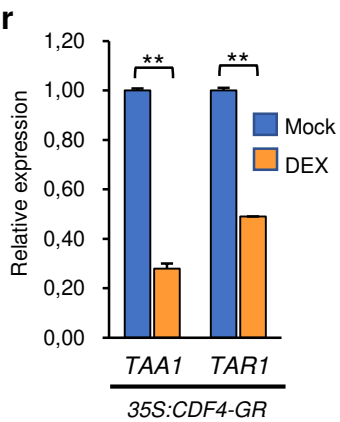
r
Relative expression
1,20
1,00
0,80
0,60
0,40
0,20
0,00
**
**
Mock
DEX
TAA1
TAR1
35S:CDF4-GR

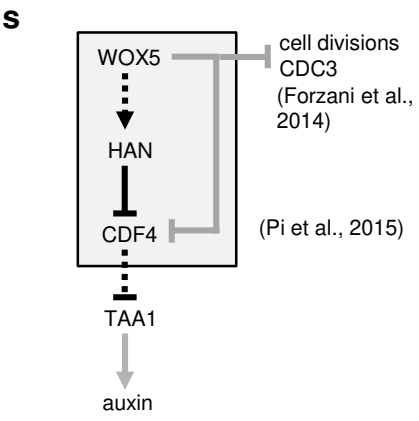
s
WOX5
HAN
CDF4
TAA1
auxin
cell divisions
CDC3
(Forzani et al., 2014)
(Pi et al., 2015)

Fig. 6: The WOX5/HAN/CDF4 cFFL regulates local auxin biosynthesis and response in the CSC niche.
a-l: Auxin response measured by *DR5:GFP* and expression of the auxin biosynthesis reporter *pTAA1:GFP-TAA1* are promoted by WOX5 and HAN and inhibited by CDF4. Representative confocal images of five-day-old seedlings from a population of atleast 15 seedlings (n>15). +DEX, 10 µM DEX induction for 24h. Insets show confocal images of GFP channel. Arrowheads indicate QC position.
m-p: Quantification of fluorescence signals of *DR5:GFP* and *pTAA1:GFP-TAA1* in the QC of the indicated genotypes. Error bars represent SD. n>15. In **m, n,** ***, $p < 0.001$, ****, $p < 0.0001$ by Student's *t*-test. In **o, p,** ****, $p < 0.0001$; by One-way ANOVA with Dunnett's multiple comparisons test.
q: Relative transcript levels of *TAA1* determined by RT-qPCR in roots of the indicated genotypes after DEX induction. Data shown are means of three independent biological replicates. Error bars denote SD. n.s., not significant, *, $p<0.05$; **, $p<0.01$; by One-way ANOVA with Tukey's multiple comparisons test.
r: Relative transcript levels of *TAA1* and *TAR1* determined by RT-qPCR in the roots of *35S:CDF4-GR* treated for 24h with either Mock or 10 µM DEX. Data shown are mean of three independent biological replicates. Error bars denote SD. **, $p<0.01$ by Student's *t*-test.
s: Model of the function of the WOX5/HAN/CDF4 module in stem cell regulation. Solid lines, direct regulation, dashed lines, indirect regulation. Black lines, this study; grey lines, indicated previous studies.
Scale bars: 20 µm.

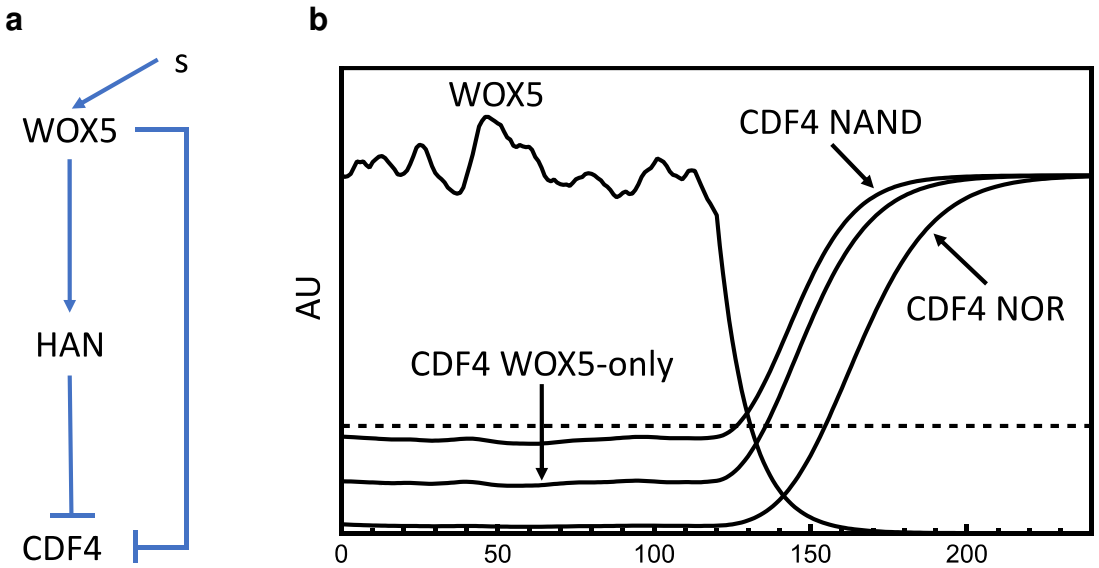

Extended Data Fig. 8 Mathematical modeling of the WOX5/HAN/CDF4 cFFL suggests a mechanism to buffer CSC maintenance against input noises.
a: the coherent feed-forward loop (cFFL) with the input signal s.
b: Results of the simulation of the network motif with noisy input. The dashed line denotes a potential detection or action threshold. CDF4 NOR: wiring of the cFFL by a NOR-gate, CDF4 NAND: wiring of the cFFL by a NAND-gate, CDF4 WOX5-only: no HAN inhibition. The parameters are the same for all cases and read: $k_1 = k_2 = k_3 = k_4 = k_5 = k_6 = 0.1$ h^{-1}, $K_1 = K_2 = 6$. The signal *s(t)* into WOX5 is turned off at t = 120h.
To explore the effect of noisy input signals and a loss of signal on the cFFL motif, we modelled the network shown in panel (a) using Ordinary Differential equations:

$$\begin{aligned}\frac{dx}{dt} &= k_1 s(t) - k_2 x \\ \frac{dy}{dt} &= k_3 x - k_4 y \\ \frac{dz}{dt} &= k_5 \vec{\mathbf{l}} \cdot \vec{\mathbf{c}} - k_6 z,\end{aligned}$$

with $x \triangleq$ [WOX5], $y \triangleq$ [HAN], and z $\triangleq$ [CDF4]. The input signal *s* is modeled as a log-normally distributed stochastic variable constructed from an Ornstein-Uhlenbeck process:

$$\begin{aligned}d\mu(t) &= -\tau^{-1}\mu(t) + \sqrt{2/\tau}\varepsilon dW(t) \\ s(t) &= e^{\mu(t)-\varepsilon^2/2},\end{aligned}$$

with τ = 6h and ε = 0.2. The vector $\vec{\mathbf{c}} = (c_{00}, c_{10}, c_{01}, c_{11})$ represents the four different states of the promoter for *CDF4*. c_{00} is the state of free binding sites, i.e., neither WOX5 nor HAN is bound, c_{10} denotes the state of only WOX5 bound, etc. Using a quasi-steady state approximation, we can write for the states:

$$\begin{aligned}c_{00} &= \frac{1}{(1+K_1x)(1+K_2y)} & c_{10} &= \frac{K_1x}{(1+K_1x)(1+K_2y)} \\ c_{01} &= \frac{K_2y}{(1+K_1x)(1+K_2y)} & c_{11} &= \frac{K_1xK_2y}{(1+K_1x)(1+K_2y)}\end{aligned}$$

Extended Data Fig. 8 cont.

K_1 and K_2 are the equilibrium constants for the binding of WOX5 and HAN, respectively. The NOR-gate logic is given by $\vec{\mathbf{I}}$ = (*1, 0, 0, 0*) and a NAND-gate logic by $\vec{\mathbf{I}}$ = (*1, 1, 1, 0*).

The simulation results can be seen in panel (b). Due to the noisy input signal *s(t)*, WOX5 fluctuates. We compare three different scenarios: i) inhibition by WOX5 only (CDF4 only WOX5), ii) combining the WOX5 and HAN signal in a NOR gate (CDF4 NOR), and iii) combining the WOX5 and HAN signal in a NAND gate (CDF4 NAND). In all three cases, the motif acts as a low-pass filter, smoothing the response of CDF4. The striking difference between the different wirings is the response to a loss of WOX5: while the WOX5-only and the NAND-gate wiring behave similarly, the NOR-gate wiring shows a delayed response to the decay of WOX5. The NAND-gate exhibits the opposite behavior; the response is faster than the WOX5-only network.